STUDY INTO THE ELECTROCHEMICAL DISSOLUTION OF TIN PRESENT IN TIN-IRON ALLOYS FOR TINPLATE RECYCLING

by

Marnix Paul
4594185

In partial fulfilment of the requirements for the degree of

Master of Science
Material Science and Engineering

Supervisors:
Dr. Y. Yang, TU Delft
Dr. A. Wittebrood, TATA Steel
Dr. E. Zoestbergen, TATA Steel
Dr. A. de Vooys, TATA Steel

To be defended publicly on March 1st, 2024 at 11:00

Thesis committee:
Dr. Y. Yang, TU Delft
Dr. S. Abrahami, TU Delft
Dr. N. Dogan, TU Delft
Dr. A. Wittebrood, TATA Steel

Delft University of Technology
Faculty of Mechanical Engineering
Material Science and Engineering Program

CONTENTS

Abstract vi

Acknowledgements vii

1 Introduction 1
- 1.1 Problem statement . . . 1
- 1.2 Relevance . . . 2
  - 1.2.1 Tramp Elements in Steelmaking . . . 2
  - 1.2.2 Steel scrap in Europe . . . 3
  - 1.2.3 Industry Incentives . . . 5
- 1.3 Alloy formation . . . 5
- 1.4 Detinning in available literature . . . 9
  - 1.4.1 Chemical dissolution . . . 9
  - 1.4.2 Electrochemical dissolution . . . 13
  - 1.4.3 Tin recovery . . . 14
  - 1.4.4 Electrolytic cells . . . 15

2 Methodology 18
- 2.1 Methodology . . . 18
  - 2.1.1 Goals and Research questions . . . 19
  - 2.1.2 Experimental campaigns . . . 19
- 2.2 Cyclic Voltammetry investigation of tin and iron in literature . . . 20
  - 2.2.1 Tin in NaOH . . . 20
  - 2.2.2 Iron in NaOH . . . 22
  - 2.2.3 Tin in MSA . . . 23
- 2.3 Experimental . . . 25
  - 2.3.1 Electrolyte choice . . . 25
  - 2.3.2 Sample preparation . . . 25
  - 2.3.3 Equipment . . . 29

3 Results and discussion 34
- 3.1 Initial redox behaviour exploration . . . 34
  - 3.1.1 NaOH . . . 34
  - 3.1.2 MSA . . . 41
  - 3.1.3 Summary . . . 46
- 3.2 Redox behaviour in an alkaline electrolyte at elevated temperatures . . . 47
  - 3.2.1 Tin . . . 47
  - 3.2.2 $FeSn_2$ . . . 49
  - 3.2.3 FeSn . . . 52

3.2.4 Summary . . . 54
3.3 Selective oxidation/detinning of new scrap . . . 56
3.3.1 Reflown tinplate . . . 56
3.3.2 Alloyed tinplate . . . 57
3.3.3 Potentiostatic results vs Galvanostatic electrolysis . . . 61
3.4 Selective oxidation of EOL scrap . . . 63
3.4.1 Non heat treated pieces . . . 65
3.4.2 Heat treated pieces . . . 65
3.4.3 Summary . . . 67
3.5 Industrial application . . . 68
3.5.1 Role of lacquer . . . 68
3.5.2 Possible additives . . . 68
3.5.3 Tin recovery from anode . . . 69
3.5.4 Plant design choice . . . 71

4 Conclusions and Recommendations **73**
4.1 Conclusions . . . 73
4.2 Recommendations . . . 76

5 Annex **82**
5.1 A: FeSn and $FeSn_2$ sample trials . . . 82
5.2 B: Influence of reference electrode distance . . . 83
5.3 C: Oscilation tin in NaOH at room temp . . . 84
5.4 D: Diffusion limited regime of tin-iron alloys . . . 85
5.5 E: Additional GDOES analysis . . . 86

List of Figures

1.1 Weight% of tin in the global steel melt over time [8] . . . 2
1.2 Scrap flow in Europe 2015[11] . . . 3
1.3 Scrap Exports out of Europe in 2021[12] . . . 4
1.4 Global scrap availability over time [5] . . . 4
1.5 Power index and alloy growth rate at temperatures below 350°C [15] . . . 6
1.6 Typical current density response of reflown tinplate scrap being detinned [15] . . . 7
1.7 The impact of temperature on alloy thickness formation [15] . . . 8
1.8 Rest alloys once all Free tin and some $FeSn_2$ diffusion has taken place at 350 °C [15] . . . 8
1.9 Pourbaix diagram for iron (black) and tin (blue) superimposed. [16] . . . 9
1.10 Basic schematic of an electrolytic cell . . . 16

2.1 Cyclic voltogramm of tin in NaOH [45] . . . 21

2.2 Cyclic voltogramm of tin in NaOH at various temperatures [45] 22
2.3 Cyclic voltogramm of iron in NaOH over multiple cycles [52] 23
2.4 Cyclic voltogramm of tin in MSA [53] 24
2.5 Elecrolyte make up for Figure 2.4 [53] 24
2.6 Binary phase diagram Fe-Sn [9] 25
2.7 X-ray Defraction analysis of the FeSn and $FeSn_2$ samples 26
2.8 Tin anode polished to mirror finish 27
2.9 Cross section of sample heated at 250 °C 28
2.10 SEM images of $FeSn_2$ surface 28
2.11 Cross section of of sample heated at 550 °C 29
2.12 SEM images of FeSn surface 29
2.13 Schematic representation of a three electrode cell 30
2.14 Electrolytic cell used for room temperature trials 31
2.15 Electrolytic cell used for elevated temperature trials 32
2.16 Detinning trial set up 33
2.17 Tube oven used for heat treatment 33

3.1 CV's of relevant metals in the NaOH system at 0.1M and 20 °C 35
3.2 Cyclic voltagramms of the exploratory NaOH system plotted against each other 36
3.3 Anodic sweeps of the four metals marked the CA investigated points 37
3.4 Chronoamperometry of tin in NaOH 38
3.5 Visualisation of correlation between the Cyclic Voltagramm and Chronoamperometry of Tin in NaOH 39
3.6 Chronoamperometry of blackplate in NaOH 39
3.7 Chronoamperometry plots of the inter-metallic alloys 40
3.8 CV's of studied metals in the MSA system at 0.1% and 20 °C 41
3.9 Anodic sweeps of the four metals marked the CA investigated points 43
3.10 Chronoamperometry of tin in MSA 44
3.11 Chronoamperometry of blackplate in MSA 45
3.12 Chronoamperometry plots of the inter-metallic alloys 46
3.13 Chronoamperometry of the four studied metals in a MSA electrolyte 47
3.14 Cyclic voltagram of tin at 80 °C 48
3.15 Anodic sweep of tin at elevated temperatures 48
3.16 Chronoamperometry of the anodic peak of tin in 1M NaOH at 80°C 49
3.17 Cyclic voltograms of $FeSn_2$ in 1M NaOH at 50 and 80°C 50
3.18 Investigation of the reduction peak observed at -1.0 volt for the intermetallic alloys at 80 °C 50
3.19 Current response comparison of the first and second peak of $FeSn_2$ at 80°C . 51
3.20 $FeSn_2$ held at -0.2 volt in 1M NaOH at 80°C 52
3.21 Cyclic voltograms of FeSn in 1M NaOH at 50 and 80°C 52
3.22 Current response comparison of the first and second peak of FeSn at 80°C . 53
3.23 Current density response of FeSn to -0.35 volt 1M NaOH at 80°C 54
3.24 The redox behaviour of $FeSn_2$ and FeSn over multiple cycles 55
3.25 Detinning trial of reflown tinplate 1M NaOH at 80°C 56

3.26 Reflown tinplate after the first step . . . 58
3.27 Reflown tinplate after the second step . . . 58
3.28 Surface of a $FeSn_2$ coating stripped from tin . . . 58
3.29 $FeSn_2$ coating stripped potentiostatically at -0.2 volt in 1M NaOH at 80°C . . . 58
3.30 SEM images before(top image) and after(bottom image) the detinning process . . . 59
3.31 Weight% depth profile before and after the detinning process . . . 60
3.32 Typical shape of the tin dissolution curve at fixed oxidative potential . . . 61
3.33 Typical shape of the $FeSn_2$ or FeSn dissolution curves at fixed oxidative potential . . . 61
3.34 Tin-iron alloy galvanostatically treated based on the maximum current density response . . . 62
3.35 Tin-iron alloy galvanostatically treated based on the maximum current density response . . . 62
3.36 Separated steel waste stream form municipal waste . . . 63
3.37 Three matching pair of scrap, heat treated pieces on the right side . . . 64
3.38 Set 2 after detinning. the bottom piece has undergone heat treatment . . . 66
3.39 Tin deposit after detinning trials [45] . . . 69
3.40 Cathode scraping and tin block forming process of the NOF . . . 70
3.41 Schematic of a concept for a continuous detinning line [19] . . . 71
3.42 Batch electrolysis setup . . . 72

4.1 Schematic example of a detinning line for EOL tinplate. . . . 75

5.1 Various trial attempts to create tin iron alloys . . . 82
5.2 Three Cyclic Voltagramms with differnt reference electrode distance . . . 83
5.3 Oscillating behavior of peak II of tin at room temperature . . . 84
5.4 W . . . 85
5.5 Weight% depth profile of tin-iron intermetallic alloys . . . 86
5.6 Highlighted weight% depth profile of tin-iron intermetallic alloys . . . 86

ABSTRACT

In the current industrial age the amount of secondary material resources is expected to increase at a fast rate. Within the steel supply of these secondary resources, the share of End-Of-Life(EOL) scrap will become bigger over time compared to new industrial scrap.

The waste stream of EOL steel scrap is heterogeneous and contaminated, complicating existing recycling routes used for industrial scrap. A way to combat the contamination is to apply heat treatment to the EOL scrap. This study investigates the implications of heat treatment on EOL tinplate, a tin coated steel product used for packaging.

Tin is considered a tramp element in a steel melt, thus the coating must be removed before recycling. Heat treating tinplate causes the tin coating to form an intermetallic alloy with the steel substrate, as a result tin atoms become more difficult to separate from the steel scrap product.

The reduction/oxidation behaviour of the two most prevalent tin-iron intermetallic alloys, $FeSn_2$ and FeSn, has been mapped through Cyclic Voltammetry(CV) in both an alkaline and acidic electrolyte. Pure tin and the steel substrate of tinplate scrap were similarly investigated to compare all elements in the system. The goal of the project is to achieve selective separation of tin of old tinplate scrap.

Further analysis of the anodic dissolution through ChronoAmperometry(CA) analysis allows insight in how the current response over time. Based on the CA results, a detinning process is tested over trials of new industrial scrap and EOL municipal scrap. The process has a high detinning rate for new scrap, while for EOL scrap the detinning is hindered by a presence of paint or lacquer. Trials on heat treated EOL scrap showed a small reduction of the negative impact of lacquers and paint. At the same time it was observed that most of the free tin transformed into $FeSn_2$.

The data from Cyclic Voltammetry, Chronoamperometry and detinning trials were used to propose a possible detinning line design for heat treated EOL tinplate scrap.

ACKNOWLEDGEMENTS

Completing this master's thesis has been a profoundly enriching and a journey of learning, one that would not have been possible without the support, guidance, and inspiration from a number of incredible individuals.

First and foremost, I would like to express my gratitude to Aad Wittebrood, my daily supervisor. Aad, your expertise and passion for engineering have been a constant source of inspiration to me. Your guidance has been invaluable, and I am deeply thankful for the patience, knowledge, and encouragement you have provided me throughout this process. You're style of research, and general stance in life really inspired me and is something I will remember .

I am also immensely grateful to Arnoud de Vooys, my supervisor in electrochemistry. As i knew little on the subject coming in, i am thankful to all the things you have thought me. Your insights and feedback have been crucial in shaping my work, and for that, I cannot thank you enough.

A special thank you goes to Yongxiang Yang, my supervisor from TU Delft's MSE department. The guidance has been instrumental in broadening my understanding and perspective in material science, and academics as a whole. Thank you for the supervision throughout the project!

To my friends and family, your unwavering support and belief in me have been my rock. I cannot express enough gratitude for your encouragement, understanding, and love. You have been my source of motivation and strength throughout this journey, and I am forever grateful for everything you have done for me.

This thesis stands as a testament to the collective effort and encouragement of each one of you. I am deeply honored to have had the opportunity to learn from and be supported by such remarkable individuals. Thank you for making this journey memorable and rewarding.

1

INTRODUCTION

1.1. PROBLEM STATEMENT

Global steel consumption keeps on rising, this can be attributed to the exponential growth in world population combined with the increasing rate of steel consumption per capita [1]. Growing rates of steel consumption go hand in hand with a growing rate of end of life (EOL) steel scrap. As primary steel resources deplete over time and as new environmental guidelines are put into place for the steel industry, the topic of EOL steel recycling will become even more relevant. There is a wide variety of steel packaging products that are coated with a thin tin layer. Tin-coated steel, from hereon referred as tinplate, is used for food, paint and beverage cans. The life span of these cans can range from weeks, to multiple years [2]. Once they reach their end-of-life they are discarded in mixed municipal waste, municipal waste bins designated for metals or a deposit-based collection scheme. They are separated by magnets from other materials found in solid municipal waste, and sold to refineries of steelmakers to be recycled. Problems might arise if the EOL tinplate scrap is recycled directly. Tin is a so-called 'tramp element' which has a negative impact in the material properties of steel[3]. At the present day post consumer scrap is diluted with virgin material to ensure low tramp element concentrations so that the desired material properties can be guaranteed. Over time the share of tramp elements will go up in all new steel produced, as more steelmakers will shift towrds scrap as primary resource for their product. Tin is a valuable and expensive metal for many industrial applications. To limit the increase of concentrations for tin as a tramp element a tin recovery method is necessary prior to recycling the steel scrap. A problem with the steel scrap from municipal waste, so-called post-consumer scrap, is the presence of household contamination like grease, food remains or plastic remains. This will be addressed as 'organic burden' in this report. One way of dealing with this organic burden is a heat treatment to carbonize the contaminants. This study will focus on inter metallic alloys formed on this tinplate during this heat treatment. The dissolution mechanics of tin-iron alloys are not readily available in published literature. To design a process of separating tin from the tin-iron matrix found in the alloys, the redox behaviour of these alloys will be studied and compared with the pure tin coating. This is what this study aims to do.

1

1.2. RELEVANCE

1.2.1. TRAMP ELEMENTS IN STEELMAKING

According to Engineering Dictionary a tramp element can be defined as "Contaminant in the components of a furnace charge, or in the molten metal or casting, whose presence is felt to be either unimportant or undesirable to the quality of the casting."[4]. Or in other words, any element that is present in the steel's composition which is not deliberate is considered a tramp element. For some of these tramp elements the removal process can be done through oxidation in the converter such as: P, Cr, Ti, Si, C. But elements that can not be removed this way can build up and become a problem over time, examples: Cu, Sn, Ni, Mo. At the present day when post consumer scrap recycled it is diluted with virgin material to an extend where the tramp element values are low enough so that the desired material properties can be guaranteed [5]. Without the dilution, the amount of tramp elements in the global steel melt will keep increasing. The industry will be forced to address and remove these in pre-treatment before recycling the steel or find another solution later in the steelmaking process[6]. Tin is one of these tramp elements and is considered a class 1 tramp element [7]. Class 1 tramp elements are defined as: Elements that are the primary cause of embrittlement. Small concentrations (<200 ppm) are enough to cause degradation of material properties, grain segregation or embrittlement [7]. Figure 1.1 shows a steady increase in tin found in steel recycled scrap, which is expected to only grow at a faster rate[8]. With the increase in post consumer scrap availability described in section 2.2 this rate is only expected to increase in a higher rate.

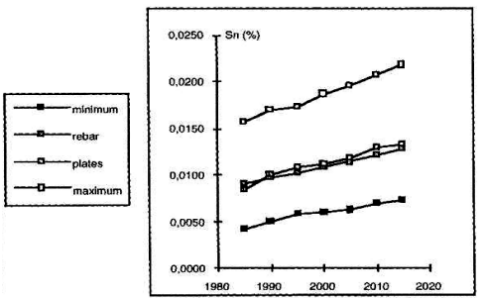

Figure 1.1: Weight% of tin in the global steel melt over time [8]

Tin as a tramp element causes unwanted phenomena during solidification or hot working of the molten steel, such as[9]:

- Solidification segregation: Due to the low melting point of tin (232 °C) relative to the molten steel temperatures (1200-1400 °C) the solidification distribution of tin will not be uniform. The variable distribution combined with the difference in solubility of the liquid and solid phases of the residual tin causes the tin to concentrate in the latter dendrites rather than the initial dendrites formed during crystallisation. This results in a heterogeneous concentration

distribution between steel and tin in the dendrite grain.

- Grain boundary segregation: Opposed to solidification segregation where the residual tin can only diffuse over a short range in a short time-span, grain boundary segregation happens over a longer interval and at a specific temperatures. It takes place at crystal defects like boundaries of recently changed phase interfaces which become enriched with the residual tin, which causes segregation. The grain boundary segregation of tin changes with the cooling rate during the continuous cooling process. This process is dynamic and consistent with non-equilibrium grain boundary segregation.

- Surface segregation: The residual tin will also be enriched at the interface of the steel and the outer oxide layer. The lower oxidation potential and melting point of tin compared to iron causes the rate of iron oxidation to be significantly higher than the diffusion rate of tin into the steel. Due to this selective oxidation, tin phases form at the interface between steel and outer oxide layer. This is especially prevalent during the high-temperature cooling and secondary heating of the steel slab.

1.2.2. STEEL SCRAP IN EUROPE

The European steel industry produces around 10 percent of the global steel production. This is around 1,885 million tonnes of crude steel and represents around €170 billion and 330 thousand people working in the industry[10]. In Europe 90% of EOL steel is collected and recycled[11]. Figure 1.2 shows what Europe's scrap flow looked like in 2015. In 2021 the EU-27 recorded a steel scrap consumption of 87.853 million tonnes in 2021 which is a 24% increase compared to 2015 [12]. In Figure 1.3 Europe's scrap export can be seen,something of note is that the Netherlands is the largest exporter of scrap to outside of the EU, and third largest inside the EU exporting around 7.7 Mt of steel scrap in total[12]. TATA Steel Europe plans to increase their scrap intake significantly over the next coming years, and aim to recycle more within the EU.

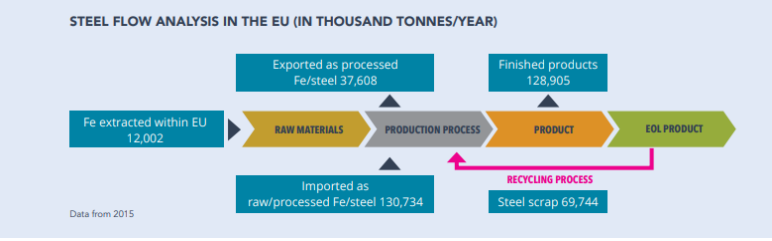

Figure 1.2: Scrap flow in Europe 2015[11]

Crude steel production has been steadily growing over time, paired with that growth comes the availability of steel scrap[5]. Scrap can be classified in three categories; fabrication scrap, production and forming scrap and post consumer scrap.

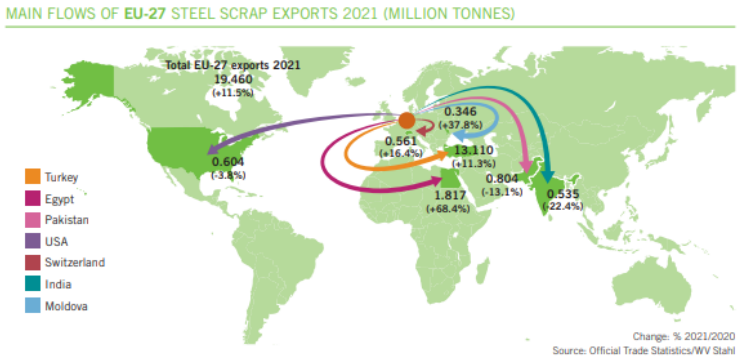

Figure 1.3: Scrap Exports out of Europe in 2021[12]

Fabrication scrap is produced internally in the steel plants, is void of contaminants and can be directly recycled in the furnace. Production and forming scrap is produced during the production of the products, for instance food cans. This scrap already has undergone treatment like coating and forming but has not entered the market, this is a homogeneous waste stream which needs minimal treatment before reintroduction into the material cycle. Post consumer scrap is scrap that has entered the market and has reached end-of-life. This last scrap type is un-characterised, heterogeneous and contaminated with organic burden. Figure 1.4 shows that post consumer scrap make up the majority of the European scrap in the future, further establishing the need for high grade recycling.

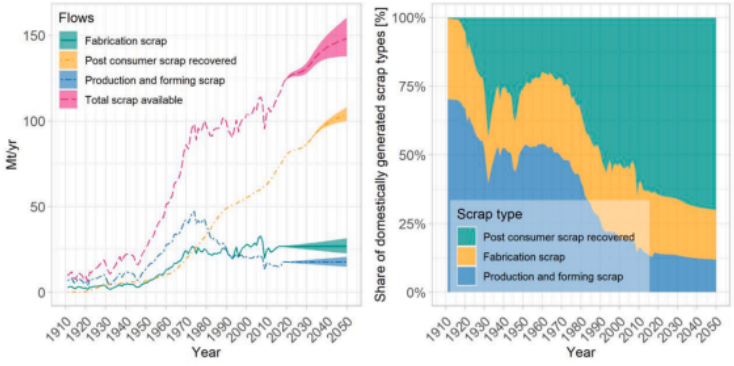

Figure 1.4: Global scrap availability over time [5]

1.2.3. INDUSTRY INCENTIVES

The European Green Deal is the future orientated plan for the EU's economy, an agenda for sustainable growth. One of the pillars of this agenda is CEAP, the Circular Economy Action Plan. In this plan they set out targets, guidelines and pan-EU agreements: "High quality recycling relies on effective separate collection of waste. To help citizens, businesses and public authorities better separate waste, the Commission will propose to harmonise separate waste collection systems. In particular, this proposal will address the most effective combinations of separate collection models, the density and accessibility of separate collection points, including in public spaces, taking account of regional and local conditions ranging from urban to outermost regions. Other aspects that facilitate consumer involvement will also be considered, such as common bin colours, harmonised symbols for key waste types, product labels, information campaigns and economic instruments. It would also seek standardisation and the use of quality management systems to assure the quality of the collected waste destined for use in products, and in particular as food contact material.[13]. This Green Deal is filled with directives and guidelines for all EU-states and the market is expected to really change shape in the next decennia.

The Netherlands has introduced a law that forces packaging companies to be responsible for the EOL processing of the packaging they produce. In 'besluit beheer verpakking 2014 – BWBR0035711' a framework and rules are set[14]. They can be summarised in a few points: 1.-Packaging industries are responsible for collection, separation and recycling of packaging waste. 2-Packaging industries are also responsible for the financial burden of said activities. 3-Packaging industries are obligated to annually report in detail how and to what extend these legal responsibilities have been fulfilled.

The law allows collective action from packaging industries, and to that purpose the 'afvalfonds' has been established. This foundation collects contributions from the packaging industries, a fixed rate per unit weight depending on the packaging material. These funds are used to pay for the activities of collection, separation and recycling of packaging waste; they have been outsourced to municipalities. The municipalities execute these activities according to the legal requirements for each material type and carefully track and report the volumes and recycling rates of the processed packaging waste in order to get reimbursed by the afvalfonds[14].

1.3. ALLOY FORMATION

Often an additional anealing treatment is applied to tinplate before being moved to production, this is knows as reflowing. Reflown tinplate has a higher corrosion resistance compared to non reflown tinplate. During the reflow step during production, a layer of $FeSn_2$ will be formed between the steel plate and the free tin. Further alloying will take place when the scrap reaches its EOL and has to be heat treated to remove any organic burden. We will look at the kinetics of this alloy formation to gain insight on the alloy formation, and how we can steer this to suit the later detinning technique.

1

The kinetics of the alloy layer on tinplate appear to follow Fick's law according to most early literature, suggesting the growth rate has a parabolic relation. However these are predominately related to the initial stages of alloy formation. On the mechanics of the free tin-alloy system after the initial formation of the alloy there has been less research, but this is much more relevant for the heat treatment that would be needed to clean EOL tinplate scrap. T.J. Chrichton has studied the effect on heat treatment on scrap and the formation of the Fe-Sn alloy system, and has found that Ficks law is not sufficient to describe its behaviour[15]. In his research it has been found that the growth behaviour of intermetallic $FeSn_2$ layer greatly depending on the temperature range, with the melting point of tin being a clear tipping point. The alloy formation rate, constant K, goes from 331 to 2000000 from just below to just above 232 °C. The temperature dependance can be seen in Figure 1.5. The activation energy for $FeSn_2$ diffusion for pre-flow melted electrolytic tinplate is $19 kJ/mol$ for temperatures below 232°C and $7 kJ/mol$ for temperatures between 232-350°C.

Temperature / °C	*Power index (n)*	*Rate constant (K)*
100	1.9	1.06
200	2.3	266
225	2.5	331
250	3.2	2.0×10^6
300	3.5	2.73×10^6
350	5.6	6.32×10^6

Figure 1.5: Power index and alloy growth rate at temperatures below 350°C [15]

In the same study by TJ Chrighton [15], unlacquered samples with a tin surface coating of 5.6 g/m2 were heat-treated in a range from 100-600 °C and were then inspected using electrochemical analysis using a potientiostat. Electrochemical stripping was carried out with an aqueous 2M NaOH solution heated to 95°C. The electrochemical dissolution profile allows for the determination of the alloy thickness by measuring the time passed between the removal of the free tin and the start of oxygen production on the base steel scrap, both are indicated by a shift in potential. An example of a typical dissolution profile of a reflowed tinplate sample can be seen in Figure 1.6.

Figure 1.7 displays the alloy growth over different temperatures. Chrichton defines three temperature regions [15]. The first region is under 232°C, here Fick's first Law of Diffusion still applies and the alloy growth rate shows parabolic behaviour with a power index of 2. For alloy layer growth the tin atoms in the free tin coating has to overcome the alloy layer that acts as a barrier between the free tin atoms and the iron substrate/alloy boundary where the alloy layer grows. This process is dependant on the presence of a free tin coating and thus the growth rate relates to the rate of tin diffusion through the alloy layer. As said before the melting point of tin really is a tipping point. When comparing temperatures immediately on either side of this point, 225°C and 250°C, it can be seen that there is almost four-fold increase in the

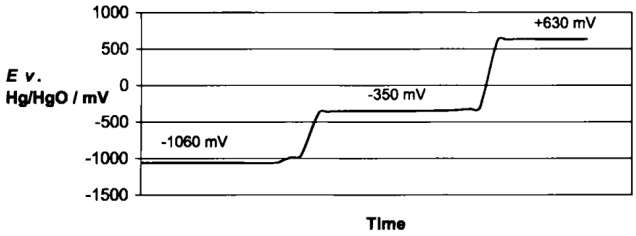

Figure 1.6: Typical current density response of reflown tinplate scrap being detinned [15]

rate of alloy formation this can be seen in the leftmost plot of Figure1.7. The second region is in the temperature range from 232°C to 350°C. The alloy growth rate can still be considered approximately parabolic, but the power index increases from 2 to 3 to 3.5 finally reaching about 5.6 as seen in Figure1.5. This can be attributed to the increased mobility of tin, significantly increasing alloy growth rates. Despite the increase, the alloy growth diffusion mechanism still obeys Fick's Law. The increase of treatment temperature from melting point to 300°C does not notably alter the method of alloy formation, but an increase to 350°C does. At this temperature an initial increase in the amount of $FeSn_2$ alloy is observed in the electrochemical stripping procedure. But this increase flattens out after around 30 min and no increase in the amount of alloy can be detected further. At 350 °C the tinplate shows a decrease in detectable $FeSn_2$ after 100 minutes, suggesting a reduction in the amount of $FeSn_2$ alloy. The third region of alloy formation starts at 350 °C and its behaviour is consistent at 400°C and above. The region is characterised by depletion of free tin, this results in a change in tinplate surface characteristics and its mechanics. Above 400 °C the electrochemical profile decreases in thickness of $FeSn_2$ alloy. In reality what happens is that the surface becomes electrochemically passive and only oxygen production takes place. Analysis by electron probe micro-analysis showed the tin to be fully distributed as a solid solution in the iron, meaning the alloy layer was completely depleted and diffused into the steel substrate. At 400°C the heating process results in an significant initial alloy formation, it is attributed to a high mobility of the molten tin. But as soon as all the initial free tin layer is depleted, the $FeSn_2$ alloy formation stops. After more time at 400 °C the apparent amount of $FeSn_2$ decreases. This pattern followed for 500 and 600 °C, but the timescale went from 10 minutes at 400°C to 2 minutes and under 1 minute respectively.

There seems to be a time delay between the depletion of the free tin and the apparent reduction in formation rate of $FeSn_2$. This is consistent with the initial $FeSn_2$ working as a barrier found in previous literature. After the tin is depleted and heat treatment above 350 °C is continued other alloys form as a result of the $FeSn_2$ alloy layer will start to form alloys with the steel substrate. These later formed alloys were measured by galvanostatic stripping to determine their potential, as can be seen in Figure1.8. If determination of the various alloy potentials in the treated tinplate is not carried out within a short time frame, then the rest potentials become

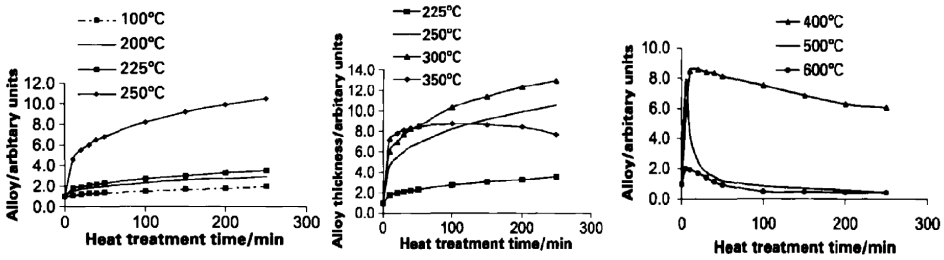

Figure 1.7: The impact of temperature on alloy thickness formation [15]

less well defined progressively over time. This is attributed to the dissociation of all but the $FeSn_2$ alloys into a solid solution of Fe in $FeSn_2$. The dissociation time is dependent on the stability per alloy. These alloys are from least stable to stable: Fe_3Sn, Fe_2Sn, Fe_3Sn_2, FeSn, $FeSn_2$. The reactions of various routes to the two most common alloys, $FeSn_2$ and FeSn, are depicted in the following reactions[15]:

$$Fe_3Sn \rightarrow Fe_2Sn + Fe \tag{1.1}$$

$$2Fe_2Sn \rightarrow Fe_3Sn_2 + Fe \tag{1.2}$$

$$Fe_3Sn_2 \rightarrow FeSn_2 + 2Fe \tag{1.3}$$

$$2FeSn \rightarrow FeSn_2 + Fe \tag{1.4}$$

Thus the most predominant intermetallic alloy is $FeSn_2$, followed by FeSn, with other negligible alloys present in very small and discrete amounts as long as the free tin is not depleted. The tin can be still recovered as an alloy as their dissolution remains Faradaic. But if alloys are dissociated into the steel, recovery of the tin is made impossible[15]. Thermal processing should ideally be restricted to temperatures below 350°C for as little time as possible to maximise the recovery of tin from used tinplate. The time is dependant of the initial amount of free tin on the surface of the tinplate. Having free tin at the surface will greatly improve the effectiveness and efficiency of electrochemical recovery of tin[15].

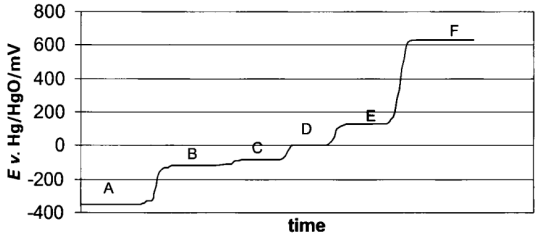

Voltage plateau	*Alloy*	*Potential v. Hg/HgO / mV*	*Electrochemical equivalent / mg C⁻¹*
A	$FeSn_2$	−350	0.507
B	FeSn	−120	0.452
C	Fe_3Sn_2	−80	0.419
D	Fe_2Sn	+5	0.397
E	Fe_3Sn	+130	0.371
F	Fe	+630	0.289

Figure 1.8: Rest alloys once all Free tin and some $FeSn_2$ diffusion has taken place at 350 °C [15]

1.4. DETINNING IN AVAILABLE LITERATURE

1.4.1. CHEMICAL DISSOLUTION

There are many ways to remove tin from its steel substrate. A range of techniques have been studied and numerous patents have been filed over the years. This subchapter will investigate what has been tried in the past. To dissolve tin into its ionic form strong bases or acids can be used, this makes sense when the Pourbaix diagram is studied in Figure 1.9, where both iron and tin are shown in black and blue respectively. Other techniques might exploit the chemical affinity between tin and the element.

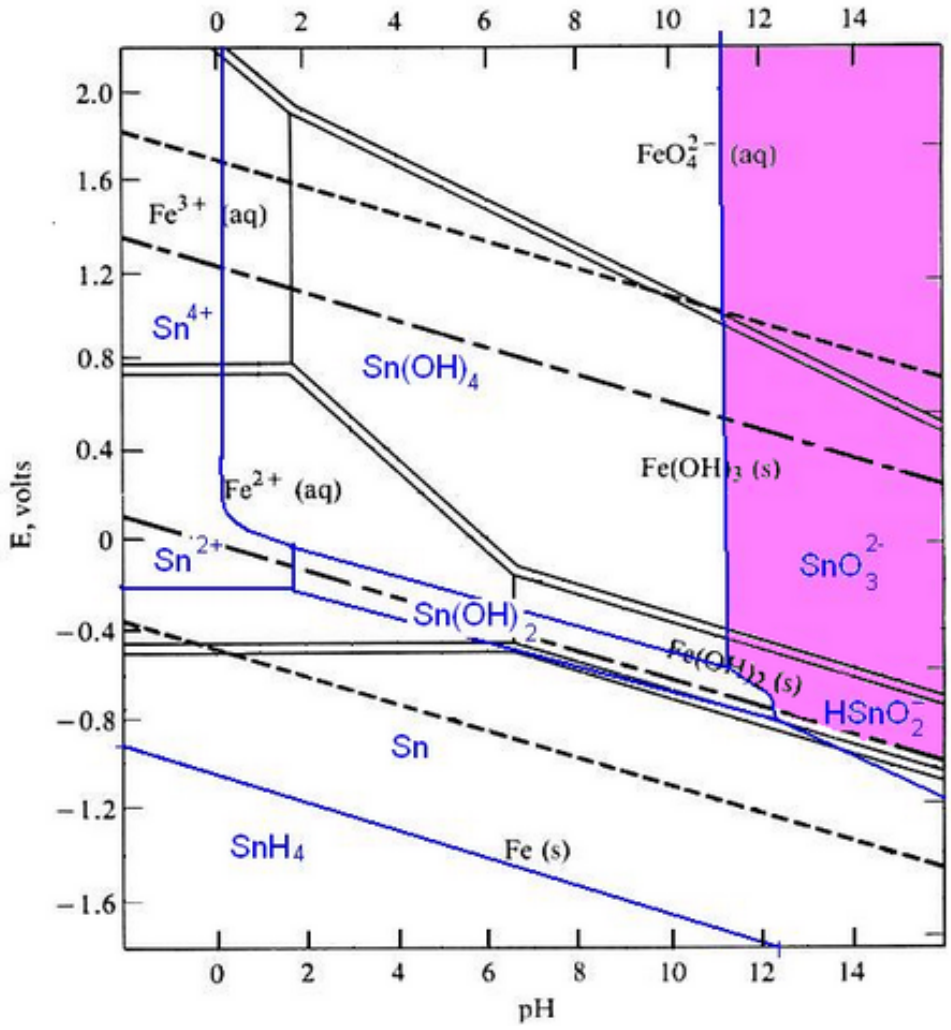

Figure 1.9: Pourbaix diagram for iron (black) and tin (blue) superimposed. [16]

The definition of dissolution is as follows: "Dissolution is the process where a solute in gaseous, liquid, or solid phase dissolves in a solvent to form a solution." [17]. In the application for detinning you ideally want to dissolve the solid tin into a liquid solution to separate it from the iron substrate that remains solid. As shown in Figure1.9 in a window of very low and high pH, thus strong acid or base, tin can be stabilised in a solution.

1.4.1.1. ACIDIC LEACHING DETINNING

A problem with acidic detinning is that the acid will also attack the underlying substrate

NEN Standard for detinning tinplate The NEN standards will serve as a starting point, in the NEN standards file (NEN-EN-10202) on tinplate they suggest a chemical removal method for the tin coating. The file has a broad range of information on cold reduced tinmill products- Electrolytic tinplate and electrolytic chromium coated steel. This norm is on the removal of the tin coating which can be useful to set a baseline before testing, to compare changes over time in the steel strip underneath the tin coating. The procedure consists of a strong acid to attack the tin layer, and an inhibitor to protect the steel: "Completely immerse the clean dry specimen in Clarke's solution. When reaction at the specimen surface ceases and a fine, uniform, black deposit of antimony is observed on the surface, wash thoroughly in hot water and brush the surface to remove the deposit. Immerse the specimen in methylated spirits, dry and store in readiness for further testing. Clarke's solution is prepared in the following manner: "Dissolve 78 g of antimony trichloride in 1 l of hot hydrochloric acid. Filter through four No 40 filter papers. Cool and dilute to 2.5 l with cold hydrochloric acid."[18]

Hydrochloric acid Hydrochloric acid is one of the more obvious acid choices for chemical detinning, as tin and chloride have a large affinity, and tinchloride is a chemical which is used in many types of industry. There are two ways the two elements tend to react in a solution, depending on the acid concentration. Respectively the reactions in strong and diluted acid[19]:

$$Sn + 4HCl \rightarrow SnCl_4 + 2H_2 \tag{1.5}$$

$$Sn + 2HCl \rightarrow SnCl_2 + H_2 \tag{1.6}$$

The first patent using hydrochloric acid dates back to 1872, and was followed by many others all adding on or varying the chemical process[20]. One mayor issue is the dissolution of iron in hydrochloric acid, this can be overcome by adding inhibitors to the solution. Patents have been filed for the following inhibitors: thiocarbanilide, antimony salts, antimony oxide, antimony trichloride, formaldehyde, glycerine foots and quinoline ethoxide [21] [22] [23] [24].

Other additives that have been tried in the past are oxidants, the reason for addition of an oxidising agent is to increase activity, reduce the liquor content time and so improving the throughput rate[19]. The most obvious available oxidant is

oxygen, which can be sourced from air. Other oxidants that have been patented are transition metal chlorides, such as ferric chloride and chromic chloride or other salts like sodium nitrate, sodium chlorine, sodium hypochlorite or sodium permanganate [25][26][27][28].

Sulphuric acid Sulphuric acid does not dissolve tin as quickly as hydrochloric acid does, but a few processes are investigated and patented,because of the preference for tin compared to iron[29]. Still to prevent solution of the iron multiple inhibitors have been tried: arsenious oxide, formaldehyde, glycerine foots and quinoline ethiodide [19].

Other acids Other acids like organic acids have been tried such as tartaric acid and acetic acid. Organic acids have the advantage to be less harmful to the environment which is very relevant in the current modern industrial era, as well as they are often cheaper to produce[30]. Other less environmental friendly acids, like hydrofluoric acid, have been trialled. But never saw success due to the harmful nature[19].

Assessment of acidic chemical dissolution Because most acids attack steel, an industrial scale for the acidic chemical detinning of tinplate would be very costly as the exposed steel plant would be under constant attack. Plant degrading is an issue, so is the attack on the iron scrap. By iron dissolution you lose valuable scrap material, and by doing so you also react the available acid which is intended for tin. So not only would you have iron losses, it also goes hand in hand with acid losses.

Attempts to passivate this attack will likely also passivate the attack of the intermetallic alloys such as FeSn and $FeSn_2$ which also would need to be targeted.

The addition of oxidant increases the overall efficiency of the acidic chemical detinning process, but this does not prevent with the above mentioned attack on the plant.

One advantage of the acid based chemical detinning plants is that the operating temperatures tend to be low, thus having lower energy costs and a less complex plant build.

1.4.1.2. ALKALINE LEACH DETINNING

At a pH above 12, as depicted in the pink region in Figure1.9, Tin can be stable alkali solution in the form of $HSnO_2^-$ or SnO_3^{-2} as long as there is an oxidant. In this pink region the iron is passivated and thus does not corrode. The oxidant contributes in this passivation, this way the tin can be recovered while the steel is unharmed[16].

Sodium Hydroxide Solution leaching makes use of a hot sodium-hydroxide solution to dissolve the tin of the steel scrap. The tin reacts with the solution to form the leachate Na_2SnO_3. The obtained leachate has separated the tin from the steel. The tin can be recovered by precipitation of said leachate followed by smelting, or with insoluble anodic electrolysis where the tin deposits on the anode [9], later explained in chapter 5.4. The leaching reactions look like the following:

The anodic dissolution of tin:

$$Sn = Sn^{2+} + 2e^{-} \tag{1.7}$$

The corresponding cathodic reaction:

$$0.5O_2 + H_2O + 2e- = 2OH^{-} \tag{1.8}$$

In an alkaline environment stannite ions are formed as:

$$Sn^{2+} + 3OH^{-} = HSnO_2^{-} + H_2O \tag{1.9}$$

And with the addition of oxygen these stannite ions are easily oxidesed:

$$HSnO_2^{-} + OH^{-} + 1/2O_2 = SnO_3^{2-} + H_2O \tag{1.10}$$

Combined these full process reactions look like the following:

$$Sn + 2NaOH + H_2O \rightarrow Na_2SnO_3 + 2H_2 \tag{1.11}$$

The potential favours the hydrogen product, this is the rate limiting factor and can be slow. This can be sped up by adding a oxidizing agent such as O_2 to promote the formation of Na_2SnO_3. Like so:

$$Sn + 2NaOH + O_2 \rightarrow Na_2SnO_3 + H_2O \tag{1.12}$$

The rate of this detinning will be determined by the oxidising agent, therefore a lot of different agents have been tried in the past, like lead based oxidisers like plumlbite, lead oxide and lead acetate [31][32][33]. Nitrite based oxidators like nitrate, nitrate of potassium nitrate also are quite effective [34][35][36]. Other elements with high affinity like chlorines and suphides also have been thoroughly tested, where chlorine, chlorate and persulphate showed the best results [37][38][39]. Approaches where the tinplate scrap touches other elements have been suggested, the principle is that an electrical couple is established between the metals and thus a higher rate of corrosion. This has been investigated for copper, silver, gold, magnesium, nickel or chromium [40][41] [42]. From which nickel has shown overall positive results to the detinning rates.

The dissolution speed of free tin in alkaline solutions follows a mass transfer control mechanism, however, the dissolution rate of tin in Fe–Sn alloys follows a mixed control mechanism [43]. As noted before the Fe-Sn alloys are a lot more stable and dissolution of said alloys will be slow without external stimulus. In similar conditions the apparent activation energy for dissolution for a 50% Sn / 50% $FeSn_2$ sample is almost three times as much as it is for free tin [43].

Assessment of alkaline chemical dissolution The nature of alkaline dissolution is a lot less active on iron based materials compared to acid based methods, and thus less steel would be lost to the electrolyte. Because of this the steel detinning plant will not be attacked as excessive as with those acidic methods. But because of

the lower volatility the detinning times using alkaline media are a lot longer than the acid based ones. Tin-iron alloys are also to stable to dissolve in NaOH in any industrial setting [19].

Compared to acidic dissolution in an alkaline environment iron based materuials will deissolva at a lot slower rate. This saves a lot on the initial investment as the process plant does not need extra corrossion proofing [19]. Another mayor advantage is that in alkaline media during the tin dissolution and extraction the OH^- uis regenerate [19].

1.4.2. ELECTROCHEMICAL DISSOLUTION

Electrochemical dissolution of tinplate is very similar to chemical dissolution, only corrosion happens under a applied potential. The tinplate acts as a corroding anode, and the potential can direct the corroded tin from the solution to the cathode. "Anodic dissolution is an electrochemical process in which metal dissolved from the anode and gases liberated at the cathodic electrode as well as at the anode surface and various electrochemical reactions take place in the bulk electrolyte."[44].

Electrochemical reactions can be recognised by electron exchange caused by the potential. An electrical potential is applied over two electrodes to stimulate the transfer of metal cations from the anodic tinplate to the cathode, where they are reduced to a solid metal. The applied potential must overcome the energy barriers due to polarization and ohmic losses, as well as accelerate reaction rates compared to leaching without applied potential.

In terms of power usage, working temperature, and output, acidic solutions outperform alkaline ones. Tin ions are primarily present in acid baths as Sn (II), whereas Sn (IV) is more often found in alkaline media. Meaning that the electric charge needed for cathodic deposition in acid solutions is only half what is needed compared to alkaline solutions. Operating temperatures for acidic electrolysis are generally lower and tin deposition rates are higher compared to their basic counterpart [45].

Nevertheless, alkaline electrolysis is the established method to remove tin coatings from steel scrap as the steel substrate is preserved and the basic solution helps with the removal of factory coatings like lacquer. In the Netherlands there is a company dedicated to this process, the Nederlandse OnttinFabriek (NOF) which is located in Leeuwarden and uses a variation of this method to detin clean production-and-forming scrap at an industrial scale. Alkaline solutions require a lower current density to operate and tend to be more stable. The higher operative temperatures are in place to counteract excessive hydrogen evolution and anode passivisation [45].

In an alkaline solution tin plated steel is used as an anode in combination with a iron plate as a cathode, as this makes for easy removal of the deposited tin by a manner of scraping. Examples of the electrolyte used for this process are: $NaOH$, Na_2SnO_3 or Na_2CO_3. When a direct current is applied over the pair operating at 60-80 °C, the tin will dissolve into the solution and will be deposited on the steel cathode in the form of a porous, spongy metal collected every few hours[9]. The

reactions are given below:

$$Sn + 3OH^- \rightarrow HSnO_2^- + H_2O + 2e^- \tag{1.13}$$

$$HSnO_2^- + 3OH^- + H_2O \rightarrow Sn(OH)_6^{2-} + 2e^- \tag{1.14}$$

$$2HSnO_2^- + 2H_2O \rightarrow Sn + Sn(OH)_6^{2-} \tag{1.15}$$

$$\tag{1.16}$$

At the cathode $Sn(OH)_6^{2-}$ accepts electrons and is reduced to tin:

$$Sn(OH)_6^{2-} + 4e^- \rightarrow Sn + 6OH^- \tag{1.17}$$

Just as with alkaline leaching the addition of the same oxidants has been studied. Most oxidising agents are not beneficial when an applied current is applied on the process [19]. Nitrate and nitrite are the oxidants that have shown the best improvement of results compared to other oxidants, but not in the extend that the operating temperatures of electrochemical alkaline detinning can be reduced to the level of acidic electrochemical detinning[19].

Assessment on electrochemical methods Alkaline electrochemical detinning is the state of the art in the current industry. Where alkaline leaching processes fail to target the Fe-Sn alloys present on tinplate, alkaline electrochemical processes succeed[19]. The recovery of tin in a electrochemical process is already built in, as it is deposited on the cathode through the applied potential. This can be simply scraped off and collected periodically.

Acidic electrochemical detinning is relatively less studied but has potential to outperform alkaline detinning in cost effectiveness as it requires less energy and has a higher detinning rate [45]. The issue however is the same as with the acid based leaching, the attack on the steel scrap substrate.

Overall electrochemical processes are more controllable than a pure chemical processes, as there is an extra variable to steer the process, which is either potential or applied current. And because the electric potential helps cross the energy barrier of said reactions, the operating temperature, which was the source of energy for leaching, can be lowered thus reducing costs[19].

1.4.3. TIN RECOVERY

Once the tin is removed from the steel scrap substrate by dissolution, it needs further treatment to recover a solid tin product. The electrochemical route is the most widely used method in industry, like described previously here the tin ions in the solution are dissolved by an applied potential and will deposit on the cathode in a porous form[9]. This method is the standard because it is very controllable, and the solid tin concentrates at one collection point, the cathode.

An alternative route is by crystallisation of tin in a tin rich solution. For example, by making use of the the low solubility of Na_2SnO_3 in high-concentration

NaOH solutions sodium stannate crystals were obtained by making use of the evaporation-crystallization method[46]. This can be done by keeping the solution at 80 °C, and controlling the concentration of NaOH by tracking the loss of weight of the solution until it meets requirements for further use. Similar approaches can be used for gass based separation technologies. Gassous tin can be recovered by condensation followed by crystalisation, an example of this is stannous sullfide [47]. From a solution solid tin-based particles can be precipitated or cementated under specific conditions. For example, under specific solution concentrations adding the correct ratio of iron powder grains can cause cementation of tin to take place, enabling the recovery of solid tin by filtering the solids from the solution[48]. Other techniques are solvent extraction [49], adsorption[50] and ion-exchange [51] but these are often too complex or costly to preform on an industrial scale.

1.4.4. ELECTROLYTIC CELLS

First lets do a brief summary of some of the underlying relations in electrolytic cells. An electrolytic cell is often made up of anodic and cathodic surfaces, which are electrically connected via an external circuit and submerged in an ionic conductive medium. This setup can be used to either introduce electrical energy into chemical reactions (electrolytic cell) or use chemical reactions to generate electrical energy (Galvanic cell). At the electrode/electrolyte interface, there is an exchange of electronic charges that is associated with a change in the oxidation state: oxidation reactions occur at the anode and reduction reactions occur at the cathode. Where n is the reaction's stochiometric number of electrons. The material experiences oxidation in the first reaction when it loses electrons and reduction in the second reaction when it gains electrons. It is important to note that the existence of side reactions, such as hydrogen evolution during the reduction of metallic species in electrodeposition may lower the cell's efficiency. The reactions respectively:

$$\mathrm{Me} \rightarrow \mathrm{Me}^{n+} + \mathrm{ne}^{-} \tag{1.18}$$

$$\mathrm{Me}^{n+} + \mathrm{ne}^{-} \rightarrow \mathrm{Me} \tag{1.19}$$

The standard electrode potential E^0 from the electrochemical series allows to define the cathodic and anodic reaction for a given couple.

$$\Delta E^0 = E^0_{WE/SHE} - E^0_{CE/SHE} = E^0_{\mathrm{Cathode}} - E^0_{\mathrm{Anode}} \tag{1.20}$$

For more complex systems, where temperature T and chemical activity a are relevant, the Nernst equation helps describe their relation to the potential change by comparing it to a known reference system. This equation is also one of the underlying principles of how a cyclic voltagramm is constructed. The equation:

$$E_{/ref} = E^0_{/ref} + \frac{RT}{\nu_e F} \ln \prod_i a_i^{\nu_i} \tag{1.21}$$

1

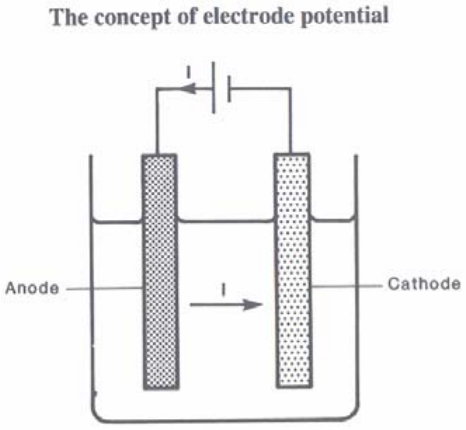

Figure 1.10: Basic schematic of an electrolytic cell

If the Gibbs free energy (G^0) is below zero the process is not considered spontaneous, and the electrochemical system is referred to as an electrolytic cell. When above zero it is considered a Galvanic cell.

$$\Delta G^0 = -nF\Delta E^0 \tag{1.22}$$

Electrolytic cells as mentioned before are used for electrode deposition. The driving force of the electrode deposition is the electrical potential (E_c) applied between the two electrodes. It causes the migration of metal cations towards the negative electrode (cathode), on the cathode the cations are reduced to the solid metallic state as a coating. The applied potential E_c should exceed the potential drops caused by ohmic losses of the electrolyte and the interfacial junction. In the formula $\eta+$ and $\eta-$ are, respectively, the anodic and cathodic over-potential $E^0_{\text{Cathode}} - E^0_{\text{Anode}}$. For the process of electrolytic detinning the tinplate is seen as the anode, from where the tin coating is stripped . The process is similar to electrorefining as the overall cell reaction is from solid metal to solid metal: Sn (anode) → Sn (cathode). This means in theory the cell potential is zero. In reality there are losses the potential has to overcome namely, Ohmic losses and Polarisation losses. Caused by the resistance of the electrolyte and wires and the formation if a charged layer that hinder ion migration, respectively.

$$E_c > \Delta E^0 + \eta_+ - \eta_- + \sum V_{\text{ohmic}} + \sum V_{\text{junction}} \tag{1.23}$$

Then Faradays law describes the theoretical amount of reactants that have undergone state change as a result to the current(I) being aplied to the anode for a set amount of time (t). In the formula n_i represents the amount of mol of material i.

$$\Delta n_i = \frac{v_i I t}{v_e F} \tag{1.24}$$

Using Faraday's law a statement can be made about the anodic current efficiency (η) of the process:

$$\eta = \frac{\Delta n^{\text{effective}}}{\Delta n^{\text{Faraday}}} \tag{1.25}$$

2

METHODOLOGY

2.1. METHODOLOGY

The main goal of this study is to derive a separation technique that attacks the tin coating and tin atoms present in the most likely intermetallic alloys; $FeSn_2$ and FeSn. The attack on the tin coating has been studied previously for clean tinplate. This study aims to evaluate the potential to detin End-Of-Life tinplate scrap which is heat-treated to remove contamination's in the form of organic burden. Due to the low melting point of tin it is safe to assume that tin-iron intermetallic alloys will be formed. The electrolytic redox behaviour of tin-iron intermetallic alloys has not been studied. To understand under what conditions a selective separation technique would preform well the redox behaviour of $FeSn_2$ and FeSn will be determined in the form of a Cyclic Voltagram.

Cyclic Voltammetry (CV) is a very popular technique in electrolytic studies, especially for the characterization of electrolytic systems. A CV measurement is a useful tool to help understand redox reactions taking place at the electrode and solution interface, as well as the kinetics of electron-transfer reaction. A Cyclic voltagram consists of a potential sweep over time and recording the current as a function of the potential. After a potential sweeping where the work electrode is charged as the anode and the oxidation reactions take place, the potential sweep is reversed and thus swept in the cathodic direction to show the reduction reactions. The characteristic currents peaks, represent the formation of the diffusion layer surrounding the electrode surface, which relate to the potential of the electrolytic reactions of interest. This will help identify both the active cathodic and anodic phase of the sample in the solution, the anodic phase being relevant for the removal of tin and tin-iron layers. The electrolytic oxidation behaviour of the materials of interest relative to the applied potential can be determined from the anodic sweeps in the Cyclic Voltagram.

However this does not give a full picture of the oxidation/dissolution versus applied potential as the potential is not constant. Chrono Amperometry(CA) is used to observe the current response to a chosen potential over an extended time. This is necessary to create a better understanding of the dominating/limiting mechanisms during the oxidation process over time.

Measuring and comparing the CV's and CA's of tin, blackplate, $FeSn_2$ and $FeSn_2$ will help design an electrolytic process that efficiently and selectively separates the tin from the iron substrate.

2.1.1. GOALS AND RESEARCH QUESTIONS

Goals for the separation process:

- The process must extract tin from the EOL scrap in a recoverable matter.
- The process must be selective, meaning minimal iron losses.
- The process must be simple and robust, complexity must be avoided.
- The process must be efficient, applied energy should go into tin removal.

Research questions to be answered:

- What is the electrolytic oxidation behaviour of tin, iron, $FeSn_2$ and FeSn?
- What type of electrolyte would be more suitable: acidic or alkaline?
- What are the limiting factors/parameters in electrolytic tin separation?
- What type of electrolytic attack would be the most effective?
- What would a potential EOL tinplate scrap detinning process line look like?

2.1.2. EXPERIMENTAL CAMPAIGNS

The experimental campaigns listed will help answer these questions, and will have a corresponding section in chapter 3.

- Initial redox behaviour exploration
- Study of redox behaviour of chosen electrolyte under operating conditions
- Selective oxidation/detinning of new scrap
- Selective oxidation/detinning of EOL heat treated scrap

Initial redox behaviour exploration : To become familiar with the systems at hand and decide with what electrolyte to continue, their redox behaviour will be mapped using cyclic voltammetry. This is done under conditions of low concentration, a small surface area and low temperatures. This is done so that only small current values are observed, and thus the measurement will have high accuracy and as little influence by ohmic drop. The CV's will give insight in passive and active oxidation regions, which is important for a selective process. As a Cyclic Voltagramm has a continuously varying potential the current density response on the y-axis is not a true representation of the current response. In a potential sweep the time-dependant factors are not taken into account. To create a better understanding the oxidation

regions of interest will be studied using Chrono Ampetommetry. This will help show a better representation of the true current density response to a selected potential, as well as determine if the conditions are accelerating or decelerating the oxidation process. From this point an electrolyte choice will be made to study closer to operating temperatures.

Study of redox behaviour of chosen electrolyte under operating conditions : After the initial study, a chosen system will be studied in futher detail. The temperature dependence will be studied by means of CV and CA similar to the first campaign. From this point an electrolytic attack on the inter-metallic alloys can be determined, as well as the mechanisms of the limitations of this attack.

Selective oxidation/detinning of new scrap : The electrolytic attack derived from the second campaign will be put to the test on new scrap. As reflown new scrap contains a layer of $FeSn_2$ a two step process can be tested to observe the difference in oxidation behaviour of the alloys and the tin. This will validate if the electrolythic attack chosen in the previous step is effective.

Selective oxidation/detinning of EOL heat treated scrap : In this campaign the chosen electrolytic attack will be tested on actual EOL scrap. This is the scrap as it would be collected from the Plastic, Metal, Drinkpak (PMD) solid waste stream, and thus contains lacquer, paint and organic burden. Half of the EOL samples will be given a heat-treatment to attack this burden, the other half will be used as a reference. These results will help determine the effectiveness of the chosen electrolytic attack.

2.2. CYCLIC VOLTAMMETRY INVESTIGATION OF TIN AND IRON IN LITERATURE

Cyclic Voltammetry is a technique which has been around as a charactaration technique for quite some time. Sodium Hydroxide is a popular electrolyte and thus the redox behaviour of both pure tin and iron have already been mapped in a cyclic voltogramm. These can be used to help predict and understand the redox behaviour of FeSn and $FeSn_2$.

2.2.1. TIN IN NAOH

In Figure 2.1 a CV of tin is shown at room temperature. Each numbered peak corresponds to a oxidation or reduction phenomena. Number 1, 2 and 3 correspond to the following oxidation reactions:oxidation of solid tin, the oxidation of SnO to SnO_3^2-, and the oxygen evolution reaction, respectively [45].

$$Sn + 2OH^- \rightarrow SnO + H_2O + 2e^- \tag{2.1}$$

$$SnO + 4OH^- + H_2O \rightarrow SnO_3^{2-} + H_2O + 2e^- \tag{2.2}$$

$$2H_2O \rightarrow 4H^+ + O_2 + 4e^- \tag{2.3}$$

As peak 2 reaches a higher current density compared to peak 1, the oxidation of Sn directly into SnO32- may take place, according to the following equation[45]:

$$Sn + 6OH^- \rightarrow SnO_3^{2-} + 3H_2O + 4e^- \tag{2.4}$$

After peak 2 has descended at around the -0.5V potential a passive region is observed by the layer of an insoluble oxide layer on the surface consisting of Sn(OH)4 or SnO.

Peak 4 and 5 are the reduction reactions of the system. Peak 4 is the reduction of dissolved tin atoms back into solid metal, and peak 5 is the hydrogen evolution. The corresponding reactions are[45]:

$$SnO_3^{2-} + 3H_2O + 4e^- \rightarrow Sn + 6OH^- \tag{2.5}$$

$$2H^+ + 2e^- \rightarrow H_2 \tag{2.6}$$

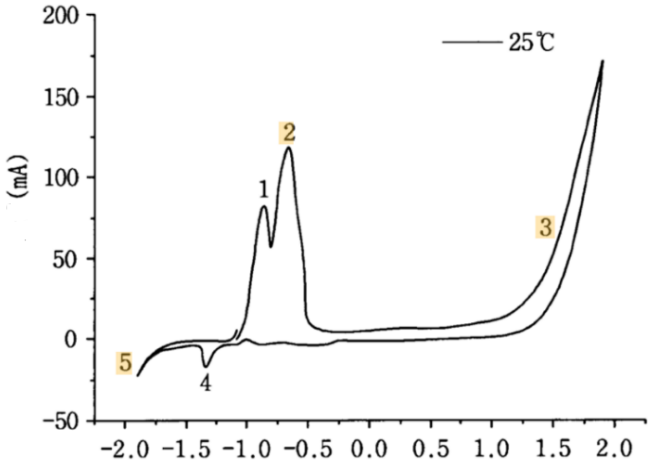

Figure 2.1: Cyclic voltogramm of tin in NaOH [45]

Peak 1 and 2 in Figure2.1 demonstrate a back and forth battle of solid tin dissolving and the dissolved tin forming an oxide layer. As a process engineer you want to minimise the possible reacting that might not be beneficial. At temperatures above 70 °C the reaction of tin dissolution overcomes the back and forth with the oxide layer formation, enabling peak 1 to rise to significantly higher current densities as seen in 2.2. Thus an increase in temperature simplifies the pure tin in NaOH system while also increasing the current density response which correlates to the detinning rate.

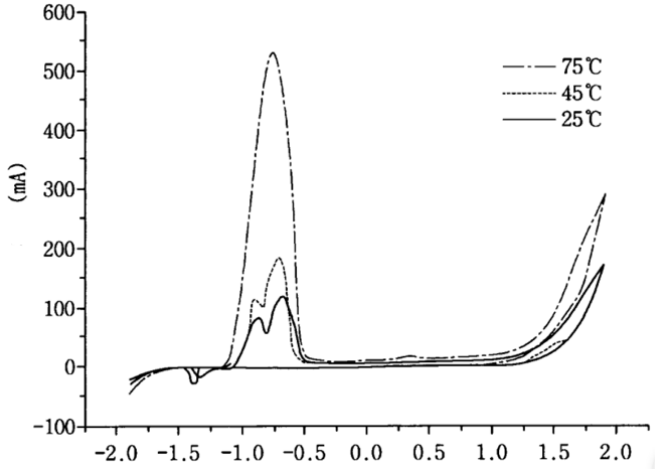

Figure 2.2: Cyclic voltogramm of tin in NaOH at various temperatures [45]

2.2.2. IRON IN NAOH

Iron is one of the most used metals worldwide and extensively researched. Figure 2.3 shows the cyclic voltogramm of iron in NaOH over multiple cycles. Note that the first scan is different in shape compared to the following scans. This is typical of the formation of an oxide layer on the surface that will not be fully reduced back to metallic state, thus acting as the new active surface in the system. The composition of this new surface layer becomes clear from the reactions associated with the peaks a1, a2 and a3. Respectively these are[52]:

$$Fe + 2H_2O \rightarrow Fe(OH)_{2\ \text{(monolayer)}} + 2H^+ + 2e^- \tag{2.7}$$

$$3Fe + 4H_2O \rightarrow Fe_3O_4 + 8H^+ + 8e^- \tag{2.8}$$

$$3Fe(OH)_2 \rightarrow Fe_3O_4 + 2H_2O + 2H^+ + 2e^- \tag{2.9}$$

The formed surface compounds of the iron are supposedly a multi-layer consisting of Fe_3O_4 and $Fe(OH)_2$.On subsequent cycles of the system a new characterisation shape is observed, with the anodic peak a4', it is theorised that the corresponding reaction is dependant on the surface layer of the oxide film and follows one of the two following reaction[52]:

$$Fe(OH)_2 \rightarrow \gamma - FeOOH + 2H_2O + H^+ + e^- \tag{2.10}$$

$$Fe_3O_4 + 2H_2O \rightarrow 3\gamma - FeOOH + H^+ + e^- \tag{2.11}$$

From Figure2.3 it is clear that from the moment the system is active an oxide film is formed on the surface which acts as a protective shield to the metallic iron. Due to this oxide layer formation, a high selectivity can be reached between tin and iron in NaOH systems, as the current density response is significantly low for iron compared to tin. This oxide layer will be addressed as ferric oxide or passive iron layer further in the report.

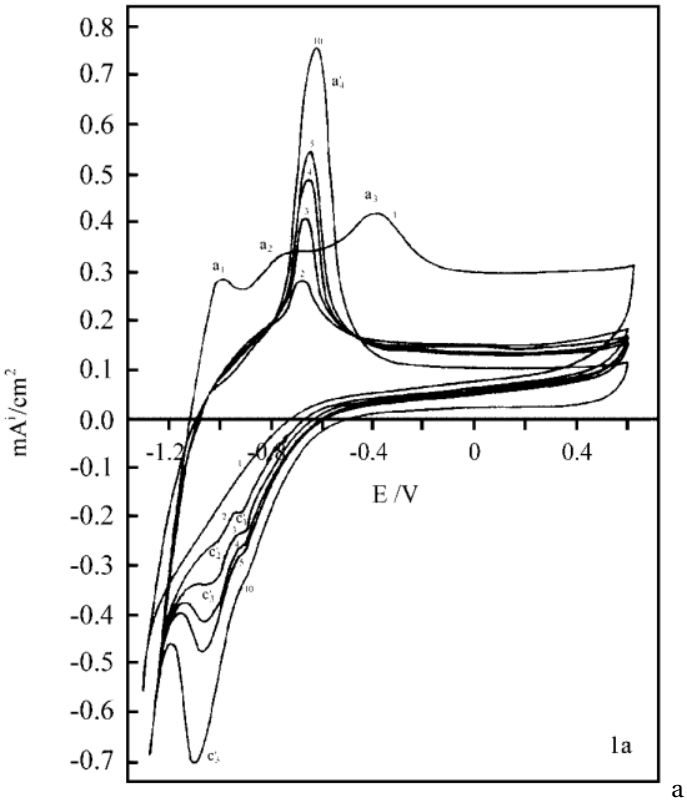

Figure 2.3: Cyclic voltogramm of iron in NaOH over multiple cycles [52]

2.2.3. TIN IN MSA

While methanesulfonic acid (MSA), CH_3SO_3H, is used in a range of industrial systems, such as the electrolyte used for applying the tin coatings. Little studies have included cyclic voltammetry to their research. No cyclic voltagramms were found of iron in MSA. For tin only one system was found, Figure 2.4 shows the CV of a system of tin in MSA system containing several additives detailed in Figure 2.5. The study was done by Low in 2008 to study the deposition of tin and copper ions which were leached from printed circuit boards as recycling method[53]. The additives were necessary to achieve the desired deposition properties of the system such as: surfactants to promote the electrode reaction, oxidation inhibitors to reduce the formation rate of stannic ion, grain refiners to produce whiskers-free or dendrite-free and brighteners to obtain matte or bright deposits. As the system is different from a tin in a pure MSA electrolyte it will be interesting to compare characteristic shape and onset of peak 1 and peak 2. In an acidic environment the reactions of peak 1

and peak 2 look like the following respectively:

$$Sn^{2+} + 2e^- \rightarrow Sn \tag{2.12}$$

$$Sn \rightarrow Sn^{2+} + 2e^- \tag{2.13}$$

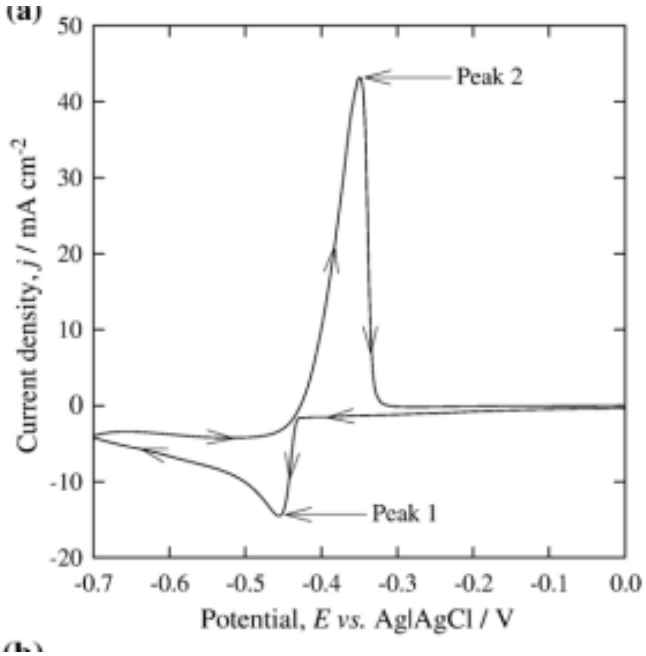

Figure 2.4: Cyclic voltogramm of tin in MSA [53]

Chemical component in the bath	Concentration in the bath	Function of the bath components
Tin(II) sulfate, $SnSO_4$	0.02 to 0.05 mol dm^{-3}	Provides Sn^{2+} for tin deposition
Copper(II) sulfate, $CuSO_4$	0.02 to 0.2 mol dm^{-3}	Provides Cu^{2+} for copper deposition
Hydroquinone, $C_6H_4(OH)_2$	0.01 mol dm^{-3}	Slows down oxidation of Sn^{2+} to Sn^{4+}
Methanesulfonic acid, CH_3SO_3H	1.9 to 2.3 mol dm^{-3}	Provides acidity and ionic conductivity
DuPont™ ForaFac® 1098	0.008 to 0.012% vol	Perfluorinated cationic surfactant as an electrolyte primary additive

Figure 2.5: Elecrolyte make up for Figure 2.4 [53]

2.3. EXPERIMENTAL

2.3.1. ELECTROLYTE CHOICE

Sodium Hydroxide (NaOH) As seen in the literature review as well in the pourbaix diagram in Figure 1.9 using an alkaline electrolyte has a large advantage of selectivity. Steel forms a passive oxide layer of $Fe(OH)_2$ protecting itself from further oxidation, while tin can dissolve as $HSnO_2^-$ or SnO_3^{2-}. But as these are unstable, they will turn into $HSnO^{2-}$ and $Sn(OH)_6^{2-}$. Under electrolytic conditions the following reactions apply[9]:

$$Sn + 3OH^- \rightarrow [HSnO_2]^- + H_2O + 2e^- \tag{2.14}$$

$$[HSnO_2]^- + 3OH^- + H_2O \rightarrow Sn(OH)_6^{2-} + 2e^- \tag{2.15}$$

Another great quality of an alkaline electrolyte for detinning is the regeneration electrolyte at the cathode of the spent electrolyte on the anode. Following the reactions:

$$Sn(OH)_6^{2-} + 4e^- \rightarrow Sn + 6OH^- \tag{2.16}$$

For these reasons NaOH is used in the operating detinning plants. Of course in practise some of the NaOH is spent, as the input material is not perfectly homogeneous. In PMD separated waste it is expected to see aluminium peel of lids that will be falsely sorted into the steel waste stream. Aluminium in NaOH is not regenerative, and will consume some of the electrolyte.

Methanesulfonic Acid (MSA) Electroplating plants that produce tinplate have been favouring methansulfonic acid (MSA) as an electrolyte of choice over the last decennia. It is a non oxidizing organic acid with a excellent solubility of metal salts, good electrolytic stabilization and conductivity, low toxicity, low costs and ease of effluent treatment as well as biodegradable disposability [54]. TATA Steel Europe is one of these producers that uses MSA therefore it is readily available and there is a intrinsic interest to find alternative uses.

2.3.2. SAMPLE PREPARATION

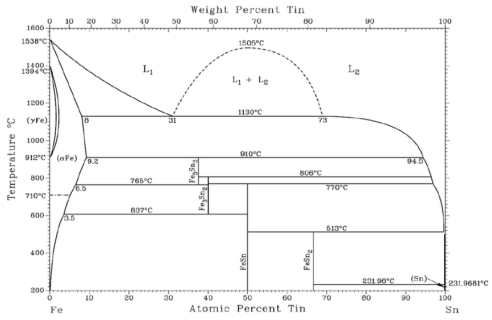

Figure 2.6: Binary phase diagram Fe-Sn [9]

2

In order to study the intermetallic alloys FeSn and $FeSn_2$ a reliable set of samples was needed. By making use of the phase diagram depicted in Figure 2.6 the correct temperature and mass:ratio can be determined. The first trials were to create a block of each intermetallic alloy to be polished after each experiment. This was unsuccessful, pictures can be found in Annex A. The approach used to create samples succesfully, is by annealing tinplate with the thickest tin coating available. Both the FeSn and $FeSn_2$ samples were prepared by annealing tinplate (TATA steel product code: 20090103) with a 11.8 (top side) 3.8 (bottom side) gr/m_2 tin coating. The top side is the side investigated and detinned. Both samples were annealed for 24 hrs, FeSn sample at 550 °C and $FeSn_2$ sample at 250 °C. Afterwards a sulfuric acid solution was used to remove the oxides formed during annealing, and the samples were rinsed with plenty of demi water.

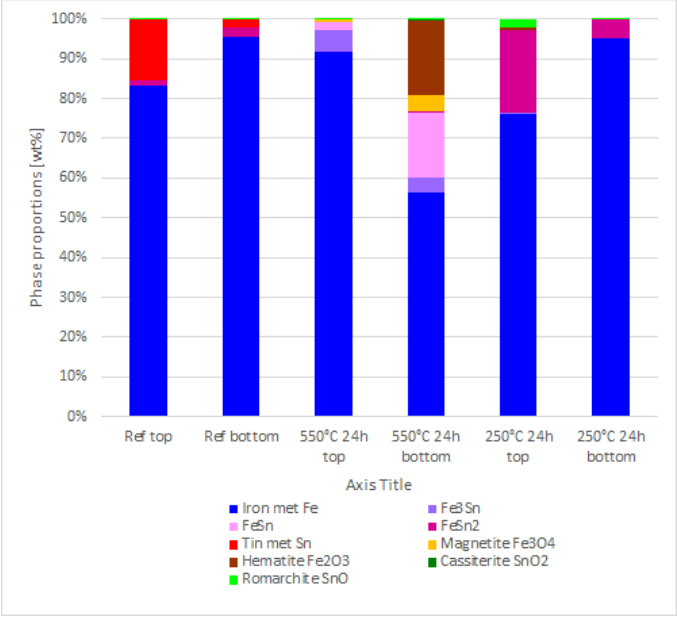

Figure 2.7: X-ray Defraction analysis of the FeSn and $FeSn_2$ samples

In Figure 2.7 the XRD analysis of the prepared intermetallic alloy samples can be seen compared to a reference sample. On the heat treated samples no free tin is available as all tin has bound with iron or has oxidised due to the heat. A lot of the tin is lost due to oxidation caused by the long heat treatment, especially for the high temperature sample. But once the oxides are removed, a steel substrate with a uniform intermetallic alloy coating is acquired.

In order to understand and compare all metals of the system, tin and steel were also studied. For tin a 99.99% pure anode was used, which was polished to a mirror finish see Figure 2.8.

To study iron, blackplate (product code: 447023) was used. Blackplate is the

substrate material on which later coatings can be applied. It is a high iron content steel with a maximum carbon content of 50 ppm. This is the best feasible representation of detinned tinplate.

Figure 2.8: Tin anode polished to mirror finish

SEM imaging The $FeSn_2$ coating formed on the sample during heat treatment at 250 °C has a thickness of 1.514μ m, as can be seen in Figure 2.9. In Figure 2.10 SEM imaging of the sample have been made. The needle like crystalines that are visible are typical for $FeSn_2$[55].

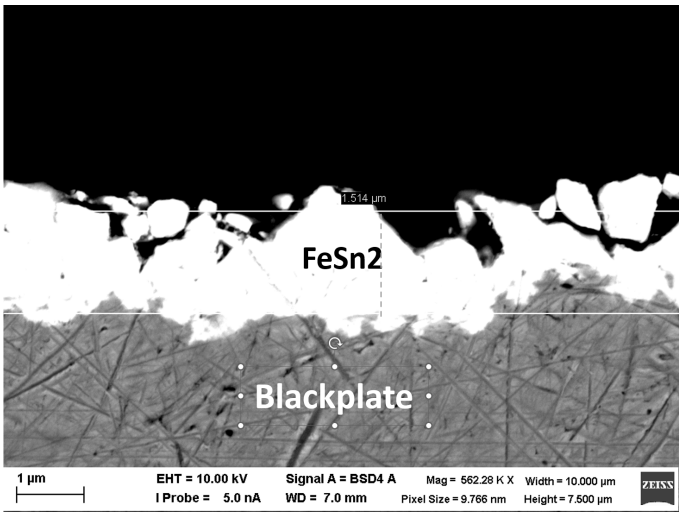

Figure 2.9: Cross section of sample heated at 250 °C

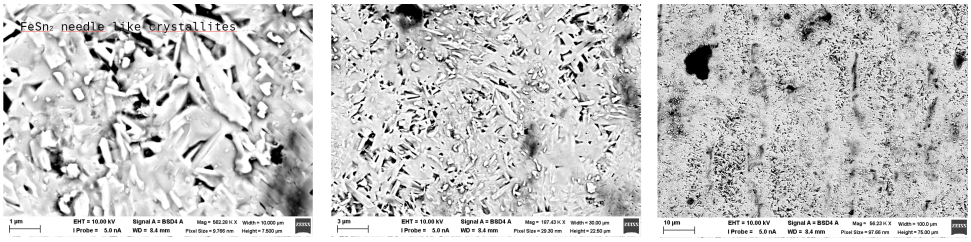

Figure 2.10: SEM images of $FeSn_2$ surface

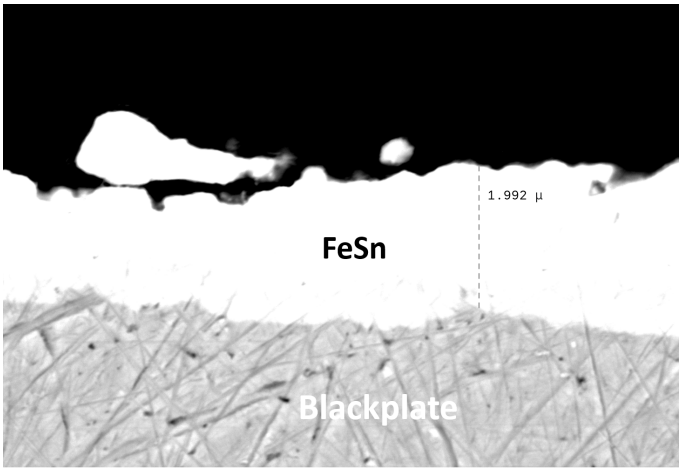

Figure 2.11: Cross section of of sample heated at 550 °C

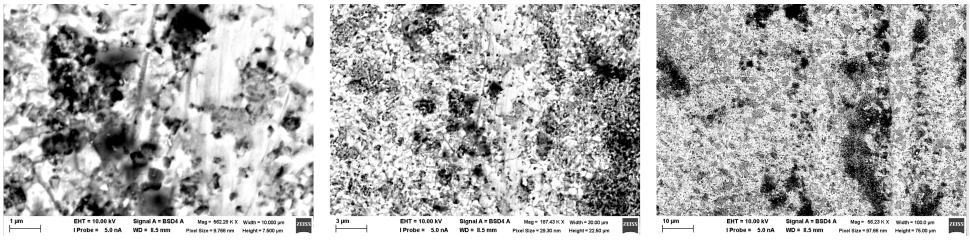

Figure 2.12: SEM images of FeSn surface

The FeSn coating on the sample formed during heat treatment at 550 °C has a thickness of 1.9924μm, as can be seen in Figure 2.11. In figure 2.12 SEM images of the FeSn coating are shown. The coating shows white tin bearing alloy grains and intergrained black areas that represent iron, a mixed interface.

2.3.3. EQUIPMENT

2.3.3.1. ELECTROCHEMICAL CELL

The first two trials performed in this study all rely on a three electrode cell setup, consisting of a working electrode, a reference electrode, and a counter electrode. Figure 2.13 shows a schematic version of the cell. For the study of the redox behaviour you want to have an as small as possible work surface. As with smaller work surface, the lower currents, the smaller the ohmic drop. And the smaller the ohmic drop the more representative the cyclic voltagramm is of the real redox behaviour. To further minimise the ohmic drop, the reference electrode should be as close to the work surface as possible. The effect of this can be seen in Annex B. During the first two characterising trials the counter electrode consists of an inert

platinum mesh, and the reference electrode used is a saturated calomel electrode. In the detinning trials the platinum mesh is exchanged for a stainless steel slab, on which the dissolved tin can be deposited. The anodes/work electrodes used are: Pure tin anode, Blackplate, $FeSn_2$ coated steel, FeSn coated steel.

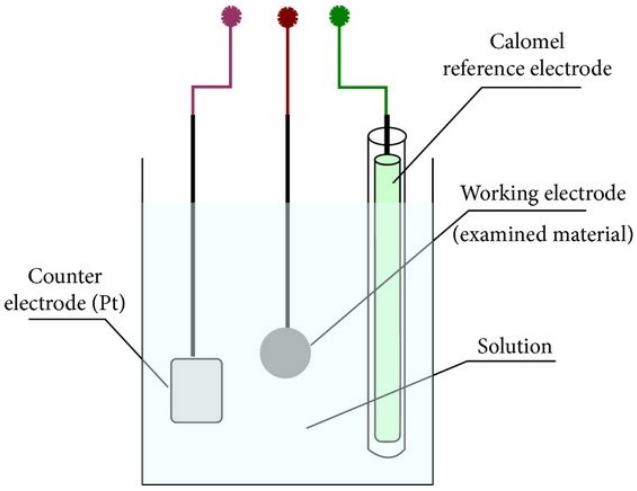

Figure 2.13: Schematic representation of a three electrode cell

Saturated calomel electrode The reference electrode used during all trials is Saturated Calomel Electrode(SCE). It is a type of reference electrode commonly used in electrolytic measurements and experiments due to its stability, wide potential range and availability. It consists of a glass tube filled with a saturated potassium chloride (KCl) solution and a silver wire coated with mercury chloride Hg_2Cl_2 immersed in the solution. The electrode's potential is determined by the equilibrium between the mercury(I) chloride and the mercury metal. Even though other reference electrodes were available,the saturated calomel electrode was selected due to being pH independent. This enables the use of the same electrode for all trials, adding to the reliability of the measurements. **All potentials mentioned in this report are measured against this SCE!!!**

Redox study at room temperature For the study at room temperature an easy to use teflon holder is used as shown in Figure 2.14. The work electrode is clamped in and fixed with screws. A small hole in the telfon holder is the an available work electrode surface of 0.42 cm^2. Work anodes used: Pure tin anode, FeSn (heat treated tinplate at 550 °C), $FeSn_2$ (heat treated tinplate at 250 °C) and blackplate. The equipment used was an AUTOLAB AUT72973 potentiostat, with a type VIRT00001 booster module. The operating software used for these trials was GPES version 4.9

(General Purpose Electrochemical System). The data was plotted using python, in a spyder IDE 5.4.5.

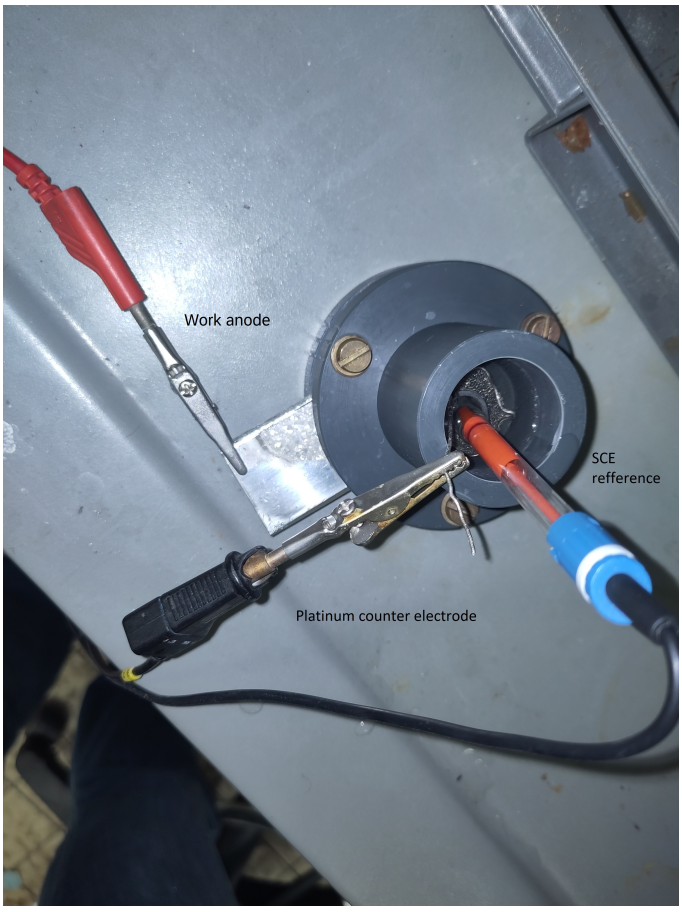

Figure 2.14: Electrolytic cell used for room temperature trials

Redox study at elevated temperatures As the electrolytic cell used for room temperature trials does not allow for a heating element due to the limited space and temperature range of the Teflon holder, another cell was used for the trials at elevated temperature. Figure 2.15 shows the inside of a double walled electrolytic cell. In the outer double wall 85 °C water is pumped around. The inside of the cell is filled with electrolyte, which is heated by the hot water being pumped around. The work anodes are made by punching a small hole in a pure tin anode, FeSn (heat treated tinplate at 550 °C), $FeSn_2$ (heat treated tinplate at 250 °C). The punched out disc can be mounted on a probe inside the electrolyte, and has an available work electrode surface of 0.7854 cm^2. The equipment used was an IVIUMnSTAT

multichannel electrochemical analyser, with the software IviumSoft 2.806. The data was plotted using python, in a spyder IDE 5.4.5.

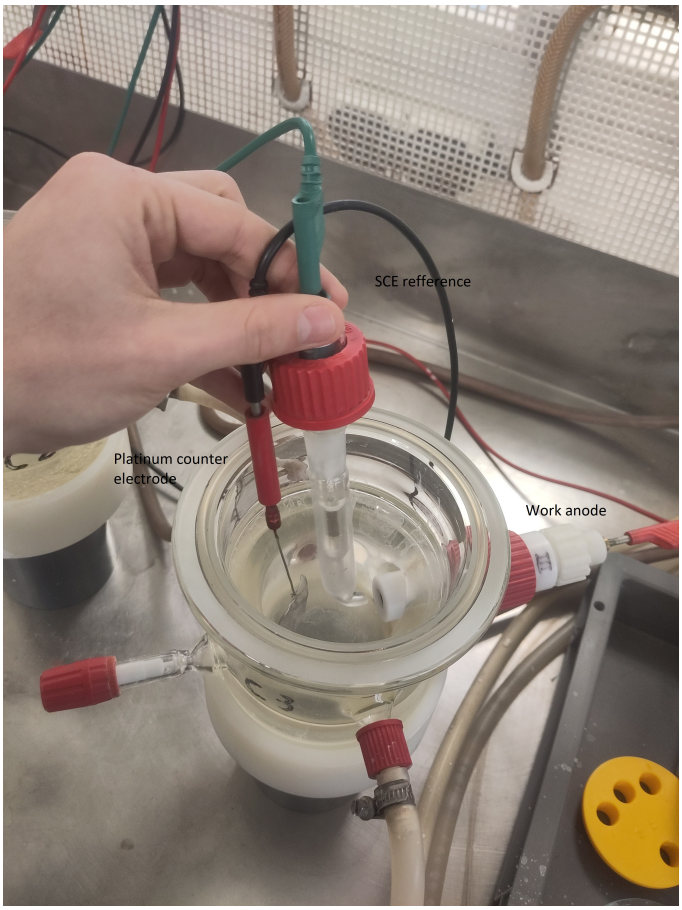

Figure 2.15: Electrolytic cell used for elevated temperature trials

Scrap detinning trials The cell used at elevated temperatures is limited by the probe work anode surface area. To detin larger pieces of scrap the setup in Figure 2.16 is used. A large glass beaker holds the electrolyte, and is heated by a hot stirrer as depicted. Both the work electrode and counter electrode are held in place by rubber tubing. The reference electrode is clamped as close as possible to the work electrode, to prevent them touching a rubber ring was used. The equipment used was an AUTOLAB AUT72973 potentiostat, with a type VIRT00001 booster module. The software used was NOVA 2.1.6. The data was plotted using python, in a spyder IDE 5.4.5.

Figure 2.16: Detinning trial set up

2.3.3.2. HEAT TREATMENT

All heat treatments were performed on a cylindrical insulated oven, as pictured in Figure 2.17. By pumping nitrogen gas through the cylinder a low oxygen atmosphere is created, to ensure tin oxidation is limited during heating.

Figure 2.17: Tube oven used for heat treatment

3

RESULTS AND DISCUSSION

3.1. INITIAL REDOX BEHAVIOUR EXPLORATION

The reduction and oxidation behaviour was first investigated in exploratory trials at room temperature and low concentrations. Based on literature, it is expected that at higher concentrations and temperatures the oxidation and reduction reactions will happen at a higher rate translating to a higher current density value, but the onset of the characteristic shapes will remain consistent. The Cyclic Voltogramms will be compared, and regions of interest will be studied with chronoampetommetry. The main regions of interest will be the steep onsets of peaks. In this exploratory phase the higher current density, the better. The Chronoamperometry measurments will give insight in the 'real' current response, as continious scanning during the cyclic voltammetry measurements gives rise to different values then a constant applied voltage.

3.1.1. NAOH

3.1.1.1. CYCLIC VOLTAMMETRY

In the alkaline system consisting of a 0.1M electrolyte of NaOH we know that iron is expected to form a passive oxide layer, while tin has a high solubility. On the following page in figure 3.1 all 4 CV's are displayed next to each other.

Tin The electrochemical anodic and cathodic behaviour of tin is mapped the Cyclic Voltagramm in 3.1a. In the anodic sweep two distinct anodic peaks are visible, marked I and II. In the cathodic sweep there is one observable reduction peak marked III. These three peaks represent the redox behaviour of pure tin in 0.1M NaOH electrolyte. The characteristic shape of this second CV cycle is consistent with those available in literature. The reactions of peak I, II and III have been described previously in section 2.2/xx. The fact that the shape is similar as observed in the literature gives validity to the setup and other measurements performed.

Blackplate The electrochemical anodic and cathodic behaviour of blackplate is mapped the Cyclic Voltagrammm in 3.1b. The anodic peak I and Cathodic peak

II are what make up the redox behaviour of the system iron in 0.1M NaOH. It is consistent with the material found in literature covered in section 2.2. Note the small current density values, especially compare to the current densities reached in the CV of tin in Figure 3.1a.

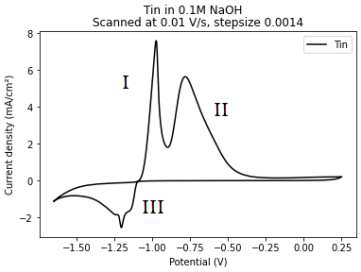

(a) CV of tin in 0.1M

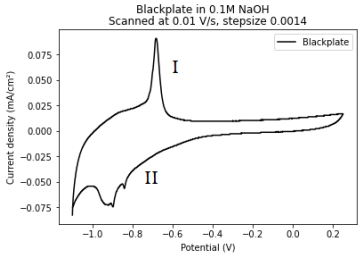

(b) CV of blackplate in 0.1M

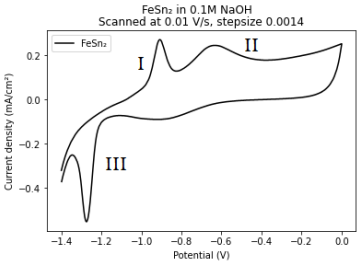

(c) CV of $FeSn_2$ in 0.1M

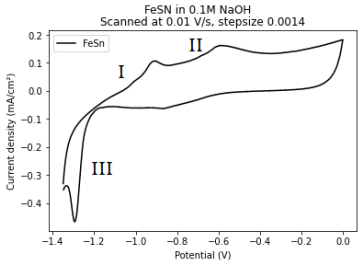

(d) CV of FeSn in 0.1 M

Figure 3.1: CV's of relevant metals in the NaOH system at 0.1M and 20 °C

$FeSn_2$ and FeSn The electrochemical anodic and cathodic behaviour of $FeSn_2$ and FeSn is mapped the Cyclic Voltagramm in figure 3.1c and 3.1d respectively. In the anodic sweep one distinct anodic peaks are visible marked I and II. In the cathodic sweep there is one observable reduction peak marked III. These three peaks represent the redox behaviour of $FeSn_2$ and FeSn in 0.1M NaOH electrolyte.

An important observation is that relative to tin, these alloys are not very active. Their active regions lay a lot closer to blackplate then they do to tin. Partly because alloys tend to have improved properties than their individual components, so will corrosion resistance often increase for alloys metals [56]. In this case, the tin that is not resistant at all, gets combined with the close-to-inert steel blackplate.

The shape of the two inter-metalic alloys is very similar, but there are some observable differences. The obvious one is that $FeSn_2$ is the more active version of FeSn. Further is the relation between peak I and peak II different for both alloys. For $FeSn_2$, the current measured for Peak I is higher than peak II. While for FeSn peak I is lower than peak II.

Under these conditions the intermetalic alloys seem to behave closer to blackplate than to tin, this is obvious when looking at Figure 3.2a where all 4 CV's are plotted in the same figure. Figure 3.2b shows that the alloys are more active than blackplate, with $FeSn_2$ slightly more active than FeSn.

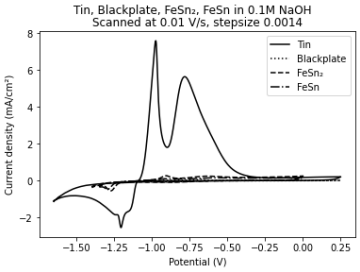

(a) CV of tin, blackplate, $FeSn_2$ and FeSn

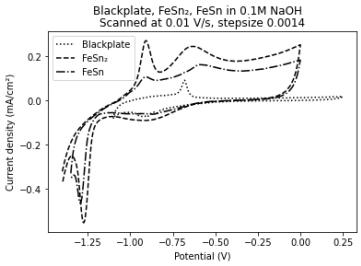

(b) CV of blackplate, $FeSn_2$ and FeSn

Figure 3.2: Cyclic voltagramms of the exploratory NaOH system plotted against each other

3.1.1.2. CHRONOAMPEROMETRY

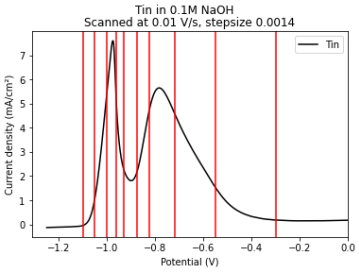

(a) Anodic sweep of tin, marked

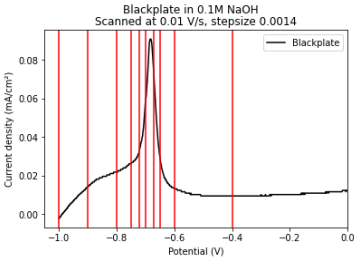

(b) Anodic sweep of blackplate, marked

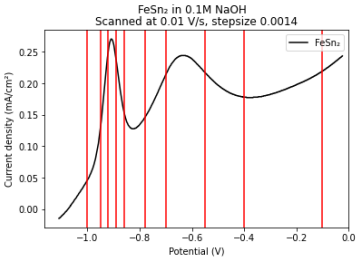

(c) Anodic sweep of $FeSn_2$, marked

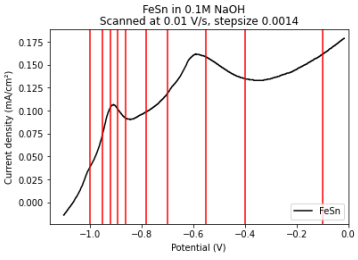

(d) Anodic sweep of FeSn, marked

Figure 3.3: Anodic sweeps of the four metals marked the CA investigated points

To understand the nature of the current density response to an applied potential the anodic sweep is isolated and marked with CA measuring points. The ascend and descent from each peak is marked with at least 3 steps during ascend and 3 steps during descend to observe the potential dependant response. The marked anodic sweeps can be seen in Figure 3.3. Each potential increase shows a sharp increase in current density only to drop afterwards. The height of the peaks vary due to a varying potential step size. The larger the step the higher the initial peak, then dropping quickly to the real system response.

Tin : In Figure 3.4 the anodic scan of pure tin, and the selected potential steps to study the anodic behaviour: (-1.1, -1.05, -1),(-0.96,-0.93),(-0.875,-0.825),(-0.72,-0.55,-0,3). Each potential is held for 30 second to reach or approach its steady state value. Figure 3.5 illustrates how these steps correspond to the peak investigation. These potential steps are grouped in 4 stages: The first peak becoming active at -1.1V, becoming passive at -1.0V, the second peak becoming active at -0.875V, and becoming passive more positive than -0.2V.

Stage 1: (-1.1, -1.05, -1) Volt, (0-90) seconds.

The first step of -1.1V, the system is reducing that is why a small deviation downwards is observed. As seen in 3.1a the onset of peak I and II are very close, a

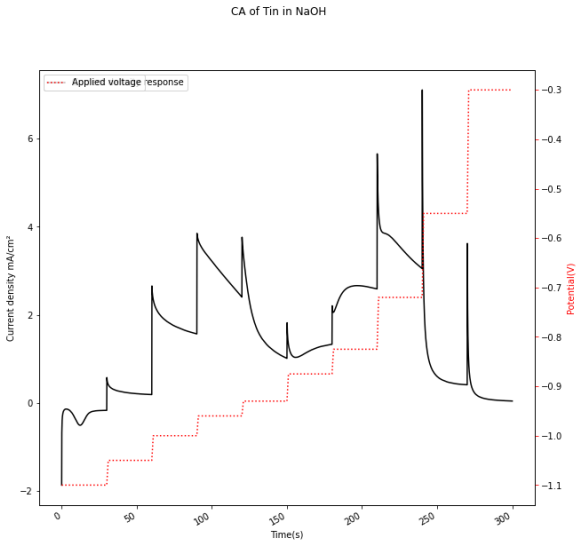

Figure 3.4: Chronoamperometry of tin in NaOH

small potential step is the difference between reducing and the oxidation window. At-1.05V and -1V steady state seems to be approached quite quickly as the current response 'flattens out' to a flat line. From that point the systems is potential steered.

Stage 2: (-0.96,-0.93) Volt, (90-150) seconds.

At -0.96V the peak has been crossed and an oxide layer is formed by the free tin reducing down on the surface, causing the decline of peak I. In the CA you can see a steady decline at this potential. Thirty seconds was not enough to even approach steady state. The same is observed for the -0.93V step. The decline of the previous step continues after a small peak caused by the voltage changing. It can be seen that the passivizing role of the oxide layer is the dominant in this potential window, as the current keeps dropping.

Stage 3: (-0.875,-0.825) Volt, (150-210) seconds.

Both -0.875V and -0.825 show an increase of current density over time showing that the potential is the dominant oxidation drive, aided by a chemical force as there is observable increase of current over time as opposed to a straight horizontal line. The small increase can be attributed to the passive tin oxide layer dissolving causing a larger amount of tin ions to release in the electrolyte.

Stage 4: (-0.72,-0.55,-0,3) volt (210-300) seconds.

At -0.72V a steep decline is observed which is in line with the passivisation of the surface causing the decline of peak II. At -0.55V and at -0.3V the current drops very quickly to 0, showing that the passive region has been reached.

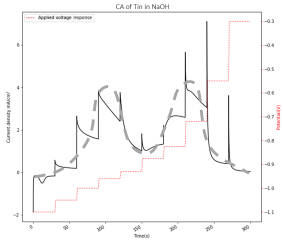

Figure 3.5: Visualisation of correlation between the Cyclic Voltagramm and Chronoamperometry of Tin in NaOH

Blackplate : For blackplate the Chronoamperometry measurements show very little other than the confirmation of expectations. Even though it appears that in the anodic sweep peak I appears to have an dissolving function. The CA measurements in Figure 3.6 confirms that iron is passive in this environment. As the current responses drop to zero and reach steady state in a very fast fashion.

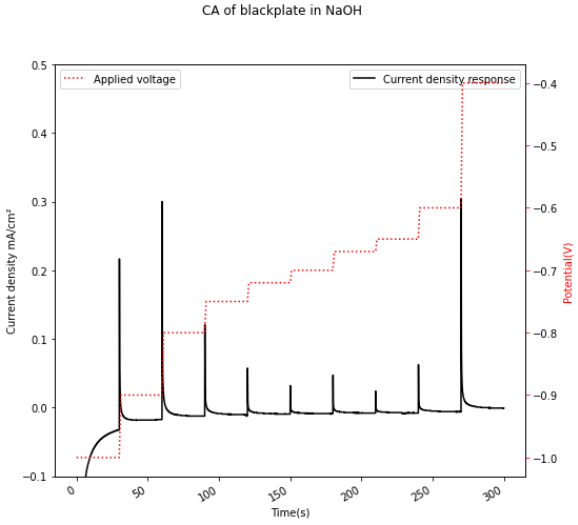

Figure 3.6: Chronoamperometry of blackplate in NaOH

$FeSn_2$ **and FeSn** :

The tin-iron alloys Chronoamperometry measurements show behaviour a lot more similar to blackplate than pure tin. Where the CA of tin clearly showed different behaviour over the 4 different phases. The CV's of the alloys also have two anodic peak in peak I and peak II, just as tin. But this is not reflected in the CA measurements. For both alloys the current responses around peak I are not really visible in the CA. The potential associated with peak I,

(-1,-0.95,-0.92),(-0.89,-0.86), show a current density that drops back to a steady state of zero in a very short time-frame. Only the later potentials associated with peak II, (0.78,-0.7),(-0.55,-0.4)(-0.1), show behaviour where the steady state is a non-zero value. So according to the CA peak II shows more dissolution compared to peak I. The currents here still show a rapid decline to a low current value, clearly showing the inert behaviour of these alloys. An electrochemical attack seems futile at room temperature, as the passive iron oxide film is dominant over the applied potential.

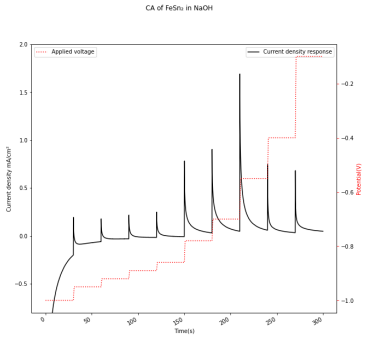

(a) CA of $FeSn_2$

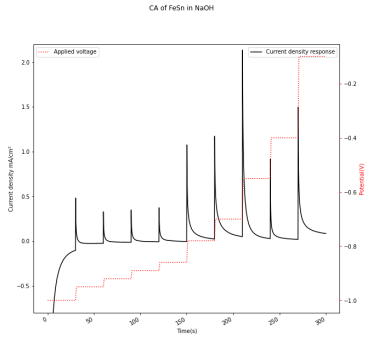

(b) CA of FeSn

Figure 3.7: Chronoamperometry plots of the inter-metallic alloys

3.1.2. MSA

In the acidic system consisting of 0.1% MSA electrolyte we expect a high solubility of tin compared to iron/blackplate. Over tin-iron intermetallic alloys in an MSA environment little available literature is published. If under these conditions the acidic electrolyte dissolves the tin atoms from the intermetallic alloys at a higher rate than iron atoms dissolve, the electrolyte is a suitable choice.

3.1.2.1. CYCLIC VOLTAMMETRY

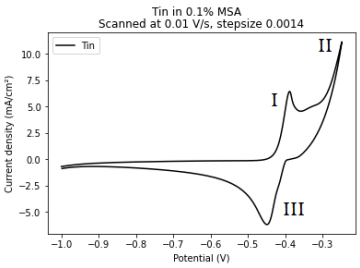

(a) CV of tin

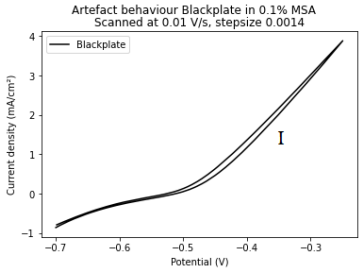

(b) CV of blackplate

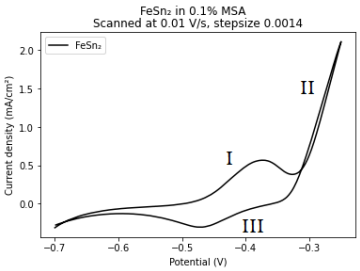

(c) CV of $FeSn_2$

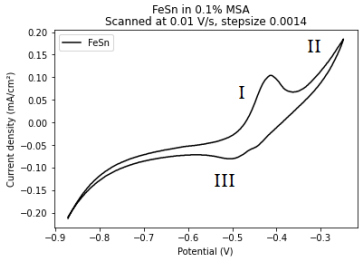

(d) CV of FeSn

Figure 3.8: CV's of studied metals in the MSA system at 0.1% and 20 °C

Tin :The electrochemical anodic and cathodic behaviour of tin in MSA is mapped the Cyclic Voltagramm in Figure 3.8a. In the anodic sweep one distinct anodic peak is visible marked I, and a purely active regime marked II. In the cathodic sweep there is one observable reduction peak marked III. These two peaks and the active regime represent the redox behaviour of pure tin in 0.1% MSA electrolyte. While tin in MSA has been studied before, the electrolyte composition was not the same. The other system found in leterature used a MSA electrolyte with cationic surfactant. This improves the reducing behaviour, but also helps tin atoms form an oxide layer to passivate the surface. This is visible in figure 2.4, due to the addatives the active region II as observed does not appear. Peak 1 in Figure 3.8a

does show some oxide layer formation causing a descent of the peak, but becomes more active as the potential is increased further. As the system of tin in pure MSA in this study is simple, the oxide layer formed in the descend of peak I is most likely Tin(II)biMethanesulfonate. As the system only exists of Tin and MSA.

Blackplate :The electrochemical anodic and cathodic behaviour of blackplate in MSA is mapped the Cyclic Voltagramm in Figure 3.8b. This CV shows no anodic of cathodic peaks, it shows an active regime marked I. This active regime represents the redox behaviour of blackplate in 0.1% MSA electrolyte. Above -0.5 volt the active regime of iron blackplate takes place. Here Iron dissolves in its divalent ionic form. Something also of note is that iron does not seem to cathodically deposit in this MSA electrolyte. This can be beneficial if the tin is electrodeposited on a steel cathode just as they do in the NOF. It appears that dissolved steel from the solution will not contaminate the tin product. As the dissolved iron is not deposited on the cathodic sweep, it is assumed that a more stable form like $C_2H_6FeO_6S_2$ will be formed [57].

$FeSn_2$ **and FeSn** : The electrochemical anodic and cathodic behaviour of $FeSn_2$ and FeSn is mapped the Cyclic Voltagramm in Figure 3.8c and 3.8d respectively. In the anodic sweep one distinct anodic peak is visible marked I and one anodic active region is observed marked II. In the cathodic sweep there is one observable reduction peak marked III. These three marked areas represent the redox behaviour of $FeSn_2$ and FeSn in 0.1% MSA electrolyte.

There is no such graph available in literature to confirm the characteristic shape. The fact that both inter-metallic alloys seem to behave in such a similar way helps argue the fact that this shape is characteristic for Sn-Fe alloys. There anodic peak followed by an active region seen in these two alloys have a similarity with the anodic behaviour of tin in MSA. And as blackplate shows no reduction in Figure 3.8b, it is assumed that the iron dissolved from the alloys also does not reduce. This implies that peak III for both $FeSn_2$ and FeSn represents tin reduction back from the electrolyte. In MSA it is again important to observe that these alloys are not very active. Alloys tend to have improved properties than their individual components, so will corrosion resistance often increase for alloys metals [56]. This can clearly be seen in these tin-iron alloys, where both the constituents are more active than both alloys. Similar as to the alkaline electrolyte the $FeSn_2$ alloy shows more active behaviour than the FeSn alloy. This makes sense as tin is more active MSA than blackplate is, thus the alloy containing more tin will be more active.

3.1.2.2. CHRONOAMPEROMETRY

To understand the nature of the current density response to an applied potential the anodic sweep is isolated and marked with CA measuring points once again. In the peaks and active regions points of interest are marked. The marked anodic sweeps can be seen in Figure 3.9. Each potential increase shows a sharp increase in current density only to drop afterwards. The height of the peaks vary due to a varying potential step size. The larger the step the higher the initial peak, then dropping quickly to the real system response.

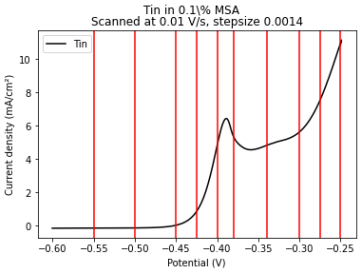

(a) Anodic sweep of tin, marked

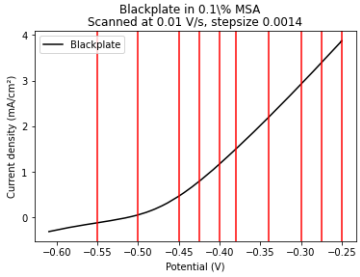

(b) Anodic sweep of blackplate, marked

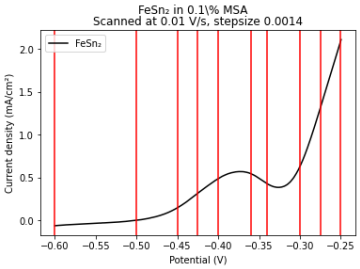

(c) Anodic sweep of $FeSn_2$, marked

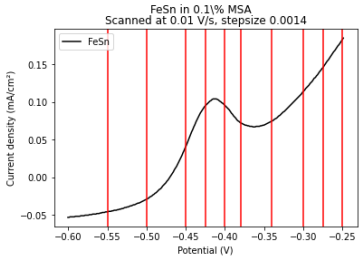

(d) Anodic sweep of FeSn, marked

Figure 3.9: Anodic sweeps of the four metals marked the CA investigated points

Tin : In Figure 3.10 below shows the current response of pure tin in 0.1% MSA over the selected potential steps to study the anodic behaviour (-0.55,-0.5)(-0.45,-0.425,-0.4)(-0.38,-0.34)(-0.3,-0.275,-0,25). Each potential is held for 30 second to reach or approach its steady state value. The ascend of peak I of pure tin in in MSA behaves quite similar to pure tin in NaOH. Once peak I's onset has started the corresponding CA steps show a decline in current density, reaching/approaching a steady state current quickly. Once a steady state has been reached the potential is the driving force. The descent of peak I due to a passive oxide layer was clear from the CA steps for the NaOH system: marked by a steep 'linear' decline angle. This is not observed in the pure tin in MSA system. The decrease in current desnity of peak I becomes less active is not directly reflected in the CA step (150-180 seconds). The potential range following this decline you would expect to see some oscilation, or signs of oxide layer forming versus direct dissolution. But all potential steps after 150 seconds show a similar decline: taking more than 30 seconds to reach steady state but seemingly all in a similar rate. The oxidation behaviour of tin in MSA electrolyse seems to be quite consistent over the active potentials. With higher current densities as the potential becomes less negative.

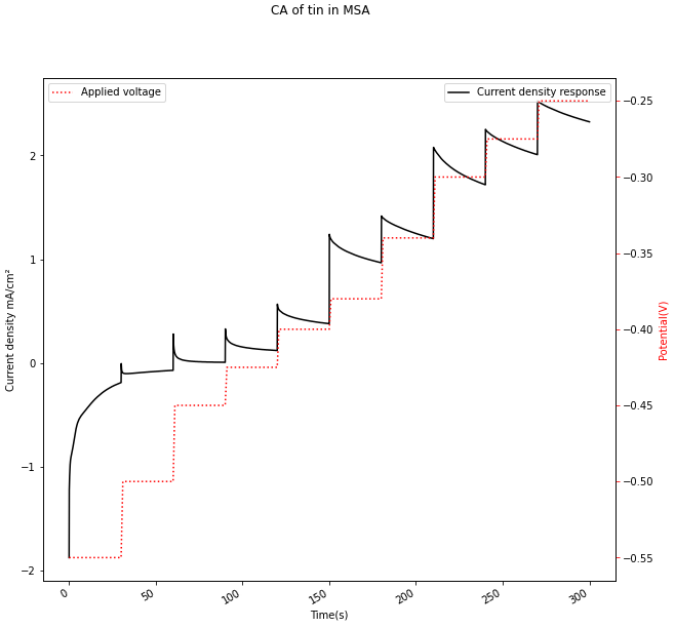

Figure 3.10: Chronoamperometry of tin in MSA

Blackplate : The figure below shows the anodic scan of blackplate in MSA, and the selected potential steps to study the anodic behaviour (-0.6,-0.5)(-0.45,-0.425,-0.4)(-0.36,-0.34)(-0.3,-0.275,-0,25). Each potential is held for 30 second to reach or approach its steady state value

Past the potential -0.5V blackplate is in an active oxidation region. The first couple of steps with a positive current density (60-120 seconds) reach a quick steady state, an oxidate purely potential driven. At higher potentials the current density only increases as the potential is held. This tells us that aside from the potential driven there is another accelerating factor, it is assumed this is the chemical dissolution of blackplate in MSA.

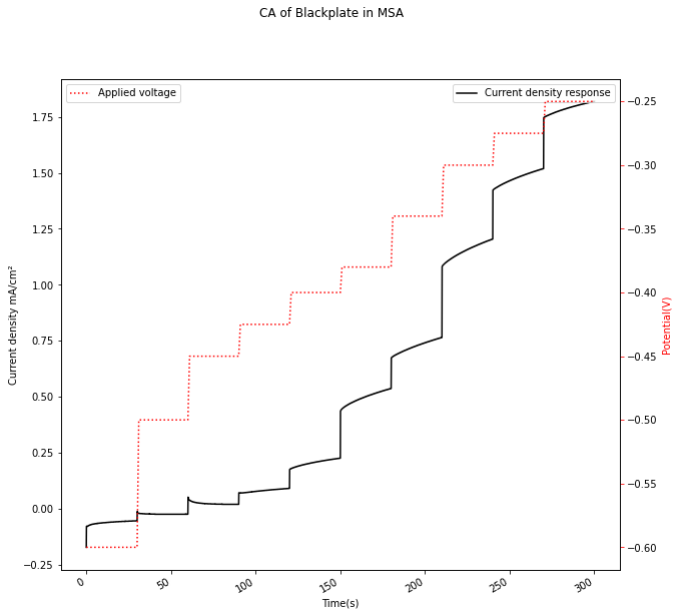

Figure 3.11: Chronoamperometry of blackplate in MSA

$FeSn_2$ **and FeSn** : The figure below shows the anodic scan of $FeSn_2$ and FeSn in MSA, and the selected potential to study the anodic behaviour (-0.6,-0.5)(-0.45,-0.425,-0.4)(-0.36/-0.38,-0.34)(-0.3,-0.275,-0,25). Each potential is held for 30 second to reach or approach its steady state value. The tin-iron alloys behave in a similar fashion to pure tin for all the potentials up until active regime II starts. Except the currents reach a steady state more quickly compare to their pure tin counterpart. Also it must be noted again that the alloys are more noble than their building counterparts, with FeSn even more noble than $FeSn_2$. As tin is still more active in MSA than iron/blackplate, this makes sense. At the more negative potentials and peak I the alloys seem to behave similar to tin, while in the active region II the later potential steps in CA show an accelerating effect in the last three CA steps for $FeSn_2$ (210-300 seconds). For FeSn only one step shows the accelerating effect, whgile further in the active regime FeSn shows purely potential driven behaviour. It is assumed that the 'accelerating effect is the chemical dissolution of tin and iron.

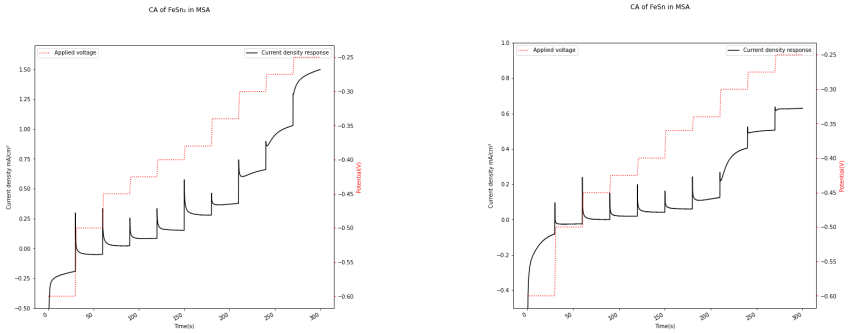

(a) CA of $FeSn_2$ (b) CA of FeSn

Figure 3.12: Chronoamperometry plots of the inter-metallic alloys

3.1.3. SUMMARY

Great selectivity is observed between tin and iron in the alkaline NaOH electrolyte. This is due to the passive iron oxide layer which is formed due to the presence of OH- in the electrolyte, and this oxide layer protects the blackplate from dissolving. Under the room temperature operating conditions the intermetallic alloys FeSn and $FeSn_2$ seemed to show passivating behaviour similar to blackplate. The free tin coating shows reactive potential driven dissolution in the onset of peak I and Peak II associated with the potentials (-1.05 to -0.95 Volt) and (-0.875 to -0.825 Volt) respectively. For a process engineer the first potential span is more desirable, as the second potential span is where passive oxide formation and dissolution oscillate or compete with each other during oxidation. This was visible during early trials as seen in Annex C, where peak II becomes unstable after a stable peak I.

In the acidic MSA electrolyte all 4 metals seem to dissolve as the applied potential shifts more positive. Figure 3.13 shows the current density response of the four studied metals plotted against eoen another with 30 second steps over the applied potentials:(-0.6,-0.5)(-0.45,-0.425,-0.4)(-0.36,-0.34)(-0.3,-0.275,-0,25). As expected in the MSA electrolyte tin seems to dissolve at a faster rate compared to blackplate. But the corrosion resistance of the two intermetallic alloys seems to be higher than the blackplate. This would imply that, if EOL tinplate is heat-treated, the steel scrap substrate would dissolve faster than the tin bearing alloyed coating. That would lead to losses of the end product of steel scrap, and would consume costly electrolyte not on detinning but scrap dissolution.

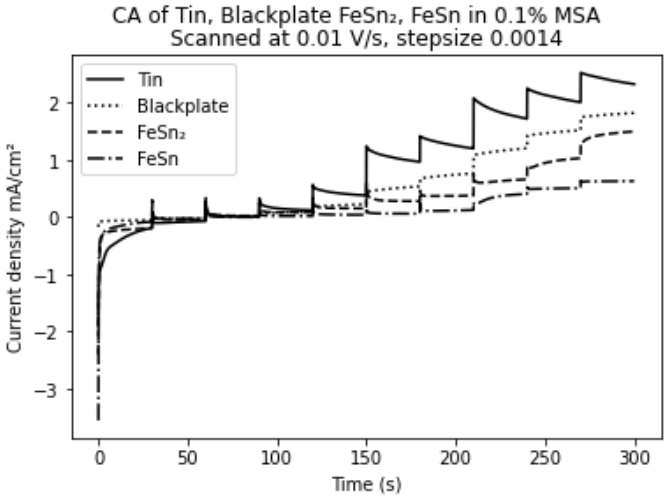

Figure 3.13: Chronoamperometry of the four studied metals in a MSA electrolyte

3.2. REDOX BEHAVIOUR IN AN ALKALINE ELECTROLYTE AT ELEVATED TEMPERATURES

A MSA electrolyte does not show a desired level of selectivity, but NaOH electrolyte does. Chronoamperometry showed that at room temperature the intermetalic alloys do not seem to show any significant signs of tin oxidation, it is expected that at elevated temperature this becomes possible due to the increase of energy by the system. Energy which is necessary for tin atoms to surpass the barrier formed by ferric oxide. This chapter investigates the redox behavior of tin, $FeSn_2$ and FeSn in an 1M alkaline electrolyte at temperatures above 70 °C. As TJ Chrighton mentioned in his PhD dissertation from 1980[19]: "Analysis of the rate of alloy electrochemical attack in most alkaline liquors, indicates that the rate is not highly dependent upon current density, but it is dependent upon temperature. In the majority of liquors the alloy will not dissolve at any appreciable rate below about 70°C".

3.2.1. TIN

As is evident in figure 2.2 an increase for temperature above 75 °C there is also a significant increase in the dissolution rate of tin. Only at high scan rates a similar cyclic voltagram was reasonably replicated, this is shown in figure 3.14. Similarly to figure 2.2 peak I and peak II of the room temperature have merged into one significantly higher peak. Though it is not a perfect replication it shows that the setup for the experiments is reliable. Due to the high scanrate the ohmic drop and current density is a lot more visible compared to the one mentioned in literature, and some form of inactivation is observed around -0.8 Volt. The reason for this is most likely that the literature uses a rotating disc while this study only uses an

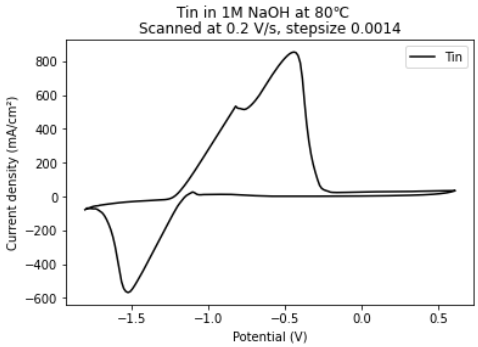

Figure 3.14: Cyclic voltagram of tin at 80 °C

exposed surface, and the high scan rate helps clear 'the vally' formed by peak I and II of tin at room temperature.

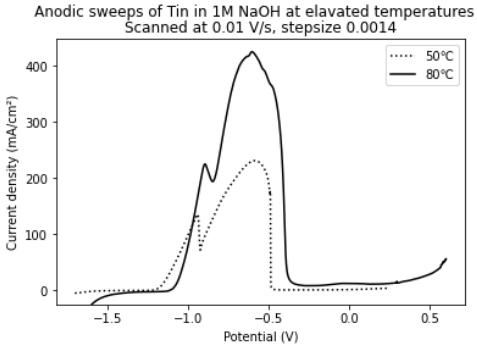

Figure 3.15: Anodic sweep of tin at elevated temperatures

The influence of temperature at a set scanrate for all the tin, $FeSn_2$ and FeSN alkaline system was studied further for both 50 and 80 °C. The anodic sweeps of tin in 1M NaOH at 80 °C are shown in figure 3.15. These sweeps are studied with Chronoamperometry shown in 3.16, with 30 second potential steps at (-0.8, -0,9, -1.0, -1.1, -1.2) volt. The first step is at the very start of the anodic peak, from this point the tin dissolution is potential driven, as the current response shows a straight line at a non-zero value. For the following steps at -0.9 and -1 volt you can also see a potential driven steady state is reached in 20 seconds. Over this part of the anodic peak follows a positive relation between the current density response and the positive shift in applied potential. The potential step of -1.1 volt shows the 'battle' of direct surface dissolution and passive oxide layer formation, as the current response shows a sharp drop halfway through the step. This indicates that the oxide layer formation has become the dominating mechanism. The last potential step's current response shoots down immediately due to the passivizing oxide layer. For

the highest dissolution rate a potential must be chosen where the potential driven dissolution is dominant with the highest current density response.

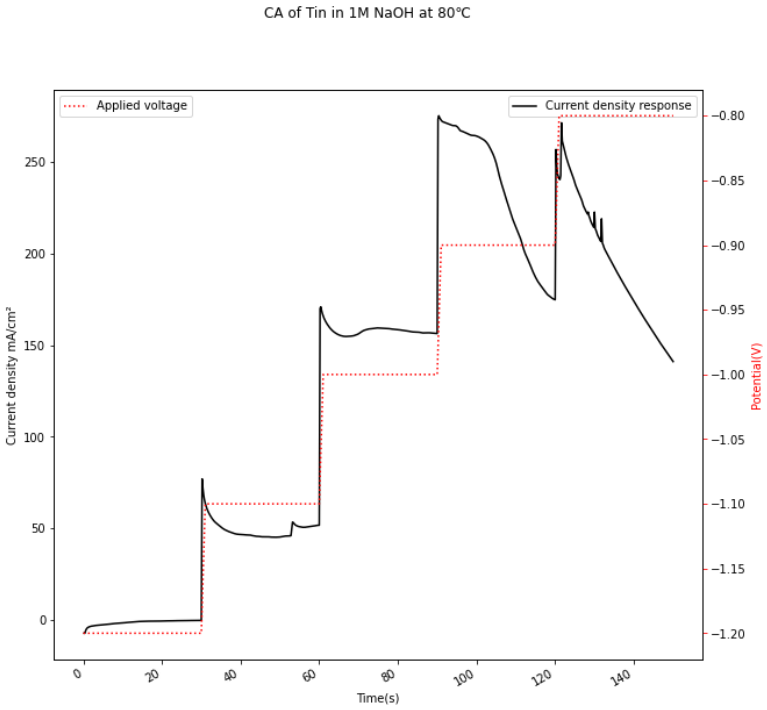

Figure 3.16: Chronoamperometry of the anodic peak of tin in 1M NaOH at 80°C

3.2.2. $FeSn_2$

The influence of the temperature increase above 70 °C can be clearly observed in Figure 3.17. Compared to the room temperature CV of $FeSn_2$ first two peaks at -0.9 and -0.6 Volt, transform in to one peak at -1.0 Volt at higher temperatures. For potentials from -0.6 volt and above a significant difference in characteristic shape is observed. At room temperature and for the 50 °C the more positive potentials in the scanned range (-1.4 to 0.0 Volt) the current density does not seem to exceed the peak around the -1.05 volt potential. The 80 °C shows a relatively large current density response approaching its maximum around 0.0 volt compared to the peak at -1.05 volt. Another observation is the additional reduction peak on the cathodic sweep. To understand if this new reduction peak is temperature dependant or caused by the new anodic rise between (-0.6 to 0.0 volt), two more CV's were performed. Visible in Figure 3.18 are two Cyclic Voltagramms, one is reversed before the onset of this anodic active region (3.18b) while the other is the full CV from hydrogen development to oxygen development (3.18a).

The fact that the reduction peak only appears when potentials above -0.6 volt

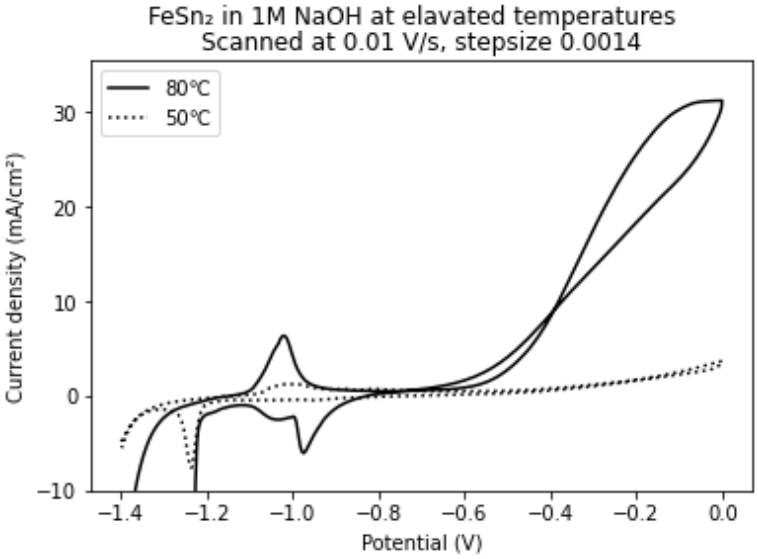

Figure 3.17: Cyclic voltograms of $FeSn_2$ in 1M NaOH at 50 and 80°C

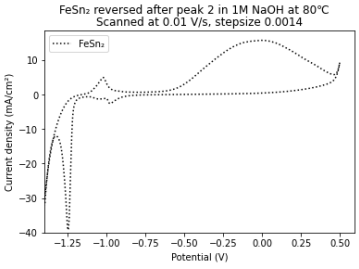

(a) CV of $FeSn_2$ sweep direction reversed at oxygen development at 0.5 Volt

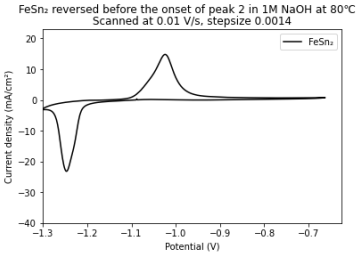

(b) CV of $FeSn_2$ sweep direction reversed before onset second anodic peak at -0.65 volt

Figure 3.18: Investigation of the reduction peak observed at -1.0 volt for the intermetallic alloys at 80 °C

have been applied, implies that from this point a different form of oxidation takes place compared to the peak at -1.05 V. This difference is further investigated with Chronoamperometry of both peaks as seen in Figure 3.19. Figure 3.19a shows the current response to the potentials (-1.05, -1.025, -1.01, -1.0) volt. The potential steps show a small current density response, which seem to reach a non-zero steady state. Compared to the CA measurements over the potentials (-0.50, -0.35, -0.20) volt shown in 3.19b, the current density values of peak 1 are significantly low. Peak

2 shows potential driven dissolution with a positive relation between shifting the potential positively and the current density response. Within this potential window the tin seems to be selectively been removed, note that this is outside the potential window where pure tin shows active dissolution.

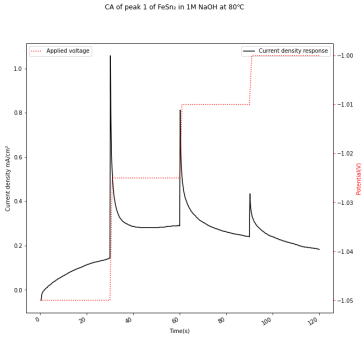

(a) Chronoamperometry investigation of peak Iof $FeSn_2$ at 80°C

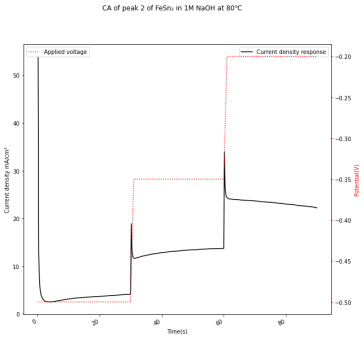

(b) Chronoamperometry investigation of peak II of $FeSn_2$ at 80°C

Figure 3.19: Current response comparison of the first and second peak of $FeSn_2$ at 80°C

To get an indication of the duration and effectiveness of detinning the $FeSn_2$ alloy one sample is held at -0.2 volt potential. Figure 3.20 shows three consecutively steps of 300 seconds combined. The effect of re-applying the potential shows in the form of a peak, but readily drops back to follow the slowly decreasing curve associated with the dissolution of tin from the $FeSn_2$ alloy. As mentioned in section 2 the surface area for this sample was 0.7854 square cm, with a $FeSn_2$ coating containing approx 10.5 gr/m^2 tin according to handheld XRF analysis. The amount of tin in the coating is approximately 0.825 mg. It took around 900 seconds to detin this surface till a steady- state like seemed to be reached. Handheld XRF analysis after treatment showed a 0.91 gr/m^2, a reduction of 91% of tin present. In repeating trials the -0.2 volt potential was held for 1500 seconds. The three repeating trials of 1500 seconds showed an average detinning percentage of 94% of tin removal. As is evident from the graph and those results, the last remaining tin contents are the hardest to remove and thus take the longest.

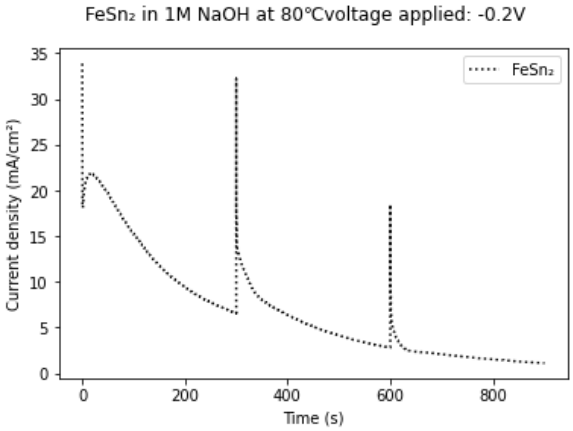

Figure 3.20: $FeSn_2$ held at -0.2 volt in 1M NaOH at 80°C

3.2.3. FESN

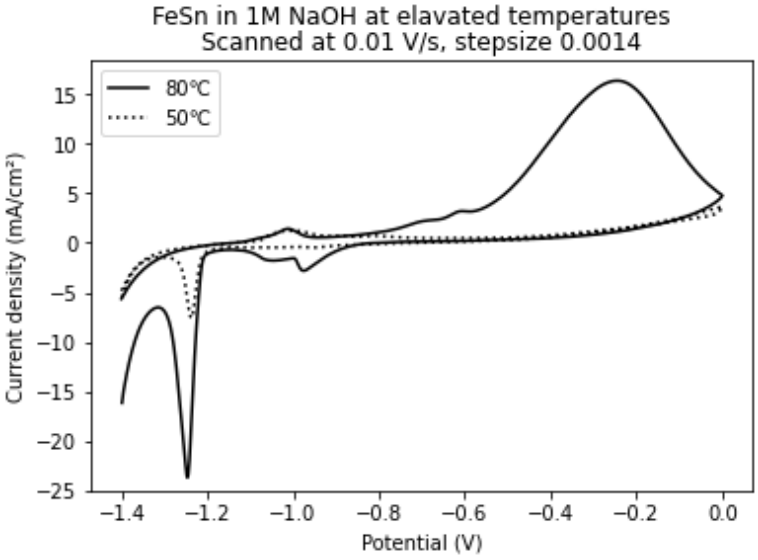

Figure 3.21: Cyclic voltograms of FeSn in 1M NaOH at 50 and 80°C

The influence of temperature for FeSn is shown in Figure 3.21. Overall the behaviour follows all the same trends as $FeSn_2$. The first two peaks at -0.9 and -0.6 Volt at room temperature, transform in to one peak at -1.0 Volt at higher temperatures. The appearance of an active anodic peak beyond the -0.6 volt potential. When both anodic peaks were studied with Chronoamperometry over the

potentials (-1.05, -1.025, -1.01, -1.0) volt and (-0.50, -0.35, -0.30) volt as seen in Figure 3.22, similar results to $FeSn_2$ were observed. The current density response to the potential steps in the first peak of FeSn seem to reach a steady state of zero, indication a quick formation of a passive oxide layer. The second peak shows signs of potential driven behaviour for the -0.50 volt step, the -0.35 volt step shows a relatively high current density response and the last step at -0.3 volt follows the decrease in current density due to a passivating oxide layer growing and covering the surface.

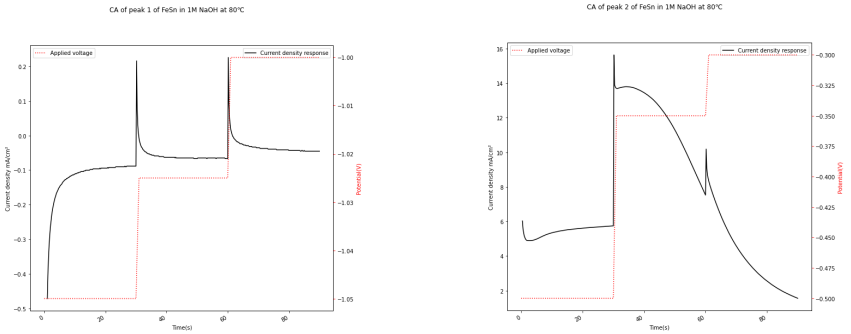

(a) Chronoamperometry investigation of peak I of FeSn at 80°C

(b) Chronoamperometry investigation of peak II of FeSn at 80°C

Figure 3.22: Current response comparison of the first and second peak of FeSn at 80°C

To investigate the detinning rate of FeSn the sample is held at a potential of -0.35V for 300 seconds. The handheld XRF analysis showed a 7.3 g/m^2 coating before detinning, with a surface area of $0.7854 cm^2$ that is approximately 0.57 mg tin is present beforehand. Figure 3.23 shows that after approx 200 seconds a steady state was reached, indicating no further dissolution. The XRF handheld read out a value of 6.2 g/m^2 indicating that there was only a 15% tin reduction of the sample. This means that once some tin has been dissolved FeSn seems to form a passive layer hindering further dissolution. It is expected that this layer is a form of ferric oxide hindering tin dissolution, it was confirmed with GDOES. FeSn might not be able to be fully detinned making use of potentiostatic detinning in an alkaline medium, due to the ferric oxides caused by the higher iron content of the alloy.

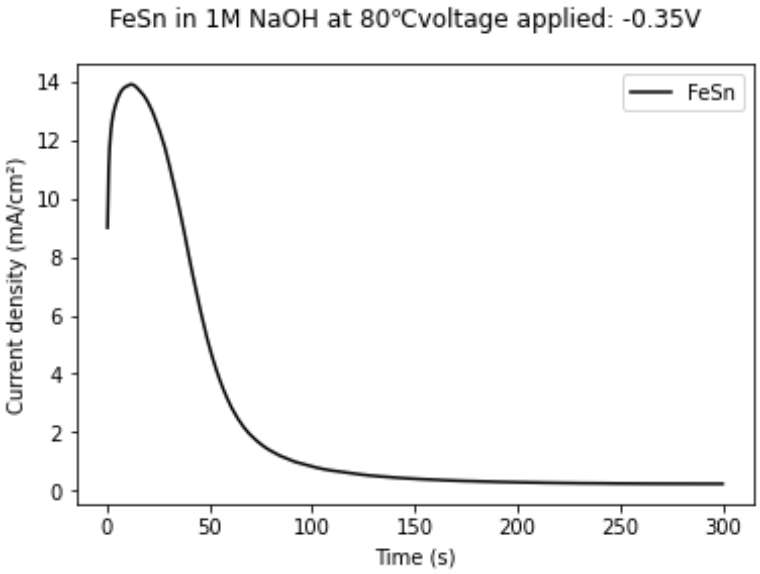

Figure 3.23: Current density response of FeSn to -0.35 volt 1M NaOH at 80°C

3.2.4. SUMMARY

The pure tin anode shows very active potential driven dissolution based on the chronoamperometry measurements. Within the active anodic area there is a positive relation between positive potential shift and current density response. Caution must be used to not shift the potential to positive, as from there passive oxide layers might be formed. Therefore the potential of -1.0 volt was selected. At a concentration of 1M and at 80 °C for an applied potential of -1.0 volt a current density response of 150 mA/cm^2 can be expected. This is a sufficiently high value for a quick detinning process as in the literature it is stated that: The current density should be in the window of 47.6 A/m^2 to 158.7 A/m^2. Optimised for energy usage, and cost efficient throughput, respectively. At the operating conditions of this study current densities 10 times higher are achieved From this it can be concluded that these conditions are suitable if current densities are limited.

For the tin-iron alloys a few new phenomena were observed for higher temperatures. The characteristic shape changes quite drastically compared to room temperature. Peak I and II at room temperature seem to merge at elevated temperatures, and a new anodic active region is observed at more positive potential values. Associated with this new active dissolution peak, is a new significantly smaller reduction peak. Chronoamperometry has shown that the peaks around -1.05 volt do not result in a steady state current density response, indicating that they represent oxidation in an other form than dissolution. This is confirmed in figure 3.24, where the alloys undergo multiple cycles of cyclic voltammetry. As can be seen the -1.05 volt peak remains similar in shape of cycles. The figure also illustrates

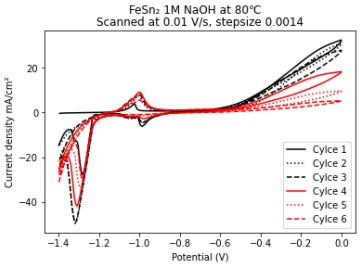

(a) Multiple cycles of $FeSn_2$ at 80°C

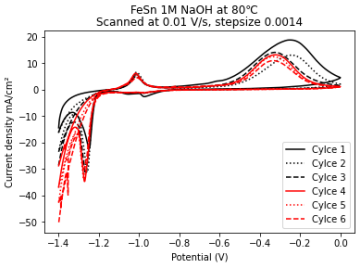

(b) Multiple cycles of FeSn at 80°C

Figure 3.24: The redox behaviour of $FeSn_2$ and FeSn over multiple cycles

that the second anodic peak decreases as the cycles continue. This is a sign of dissolved atoms being lost into the electrolyte, out of 'range' to be reduced back on the surface. As we have measured with handheld XRF the tin content decreases. This confimes the hypothesis that the -1.05 volt peak is a form of ferric oxide layer formation, while the peak with onset of -0.6V is associated with the tin dissolution out of the alloys.

Using the data collected from the cyclic voltogram and Chronoamperometry, values for detinning the $FeSn_2$ and FeSn alloys can be determined. The suitable dissolution potentials are -0.2 volt and -0.35 volt respectively. For $FeSn_2$, potentiostatic stripping with this value lead to a detinning rate of 94%, which would be increased if the electrochemical attack would be held for a longer duration. For FeSn after 150 seconds a passive oxide layer was formed, hindering the dissolution only after 15% had been dissolved. A more negative potential might be selected, that might result in a lower current density response, but will not be effected by the passive oxide layer.

Note that the active dissolution potential for tin, is in an potential window where $FeSn_2$ is not in active dissolution. And similarly for the active dissolution potential for $FeSn_2$, tin is in a passive region. Once the current response for the free tin dissolution potential (-1.0) approaches a zero value, that might be because either the substrate is blackplate or is $FeSn_2$. When that current response approaches zero, the new active dissolution potential is applied for $FeSn_2$. Once that current response drops to zero, the tin in the free tin coating and the tin-iron alloy has been dissolved.

3.3. SELECTIVE OXIDATION/DETINNING OF NEW SCRAP

By targeting the active anodic potentials of both pure tin and $FeSn_2$ a very efficient way of detinning can be achieved. Trials have been performed on reflown new scrap, the tin content of the coating is 11.8/3.8 gr/m^2 for the top and down side respectively. This tinplate is reflown, thus some of the tin coating content will already have alloyed with the steel substrate to form $FeSn_2$. XRF analysis measures that the $FeSn_2$ coating of reflown new scrap of the type used is 1 gr/m^2.

3.3.1. REFLOWN TINPLATE

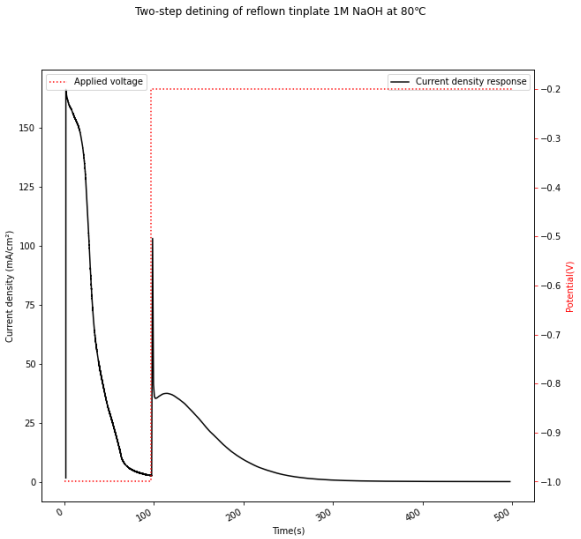

Figure 3.25: Detinning trial of reflown tinplate 1M NaOH at 80°C

Figure 3.25 displays the two step detinning process of reflown tinplate. The first step is the the free tin coating being dissolved. As the sample is submerged on both sides, the bottom side will be free of tin before the top side. This makes for the inconsistent descend of the current density response, as tin dissolution is only limited by available tin surface. Once the current density approaches zero, and thus all present free tin is dissolved, the potential is shifted to -0.2 volt to initiate the alloy attack. The alloy follows a similar current density response as observed in previously, this indicates that for the alloy attack it is not limited by the available surface coating but by diffusion. Around 300 seconds it seems that all tin is removed from the tin-iron alloy. In Figures 3.26 and 3.27 reflown tinplate is shown after the first step, and the piece of scrap after both steps of the detinning process. Figure 3.26 shows that the shiny free tin coating is removed. The dull grey surface is a 0.1 gr/m^2 $FeSn_2$ alloy layer created during the reflow process. Figure 3.27 shows the surface once this $FeSn_2$ layer has been stripped of tin. A yellow ferric oxide is visible, likely formed around the iron atoms left behind in the alloy structure.

Handheld XRF read 0.0 gr/m^2 on both the top and bottom side after the two step process was completed. Indicating a 100% removal of tin from both the free coating and the reflown alloy. The handheld XRF is not a perfect tool, thus there might be some residual tin on the samples. But even with the small error margin of the handheld XRF this easily passes tin content limits for premium scrap. By calculating the surface area under the current response (not density) the total charge can be calculated. Using the charge the efficiency can be determined by comparing the theoretical weight as a result of the charge, to the actual weight difference of the sample before and after. Making use of:

$$Q = \int_0^t I(\tau)d\tau \tag{3.1}$$

$$\Delta \mathrm{m} = \frac{MQ}{\nu_e F} \tag{3.2}$$

Over three trials an average efficiency of 92% is achieved. This is a very high efficiency, a lot higher than often seen in industrial processes. It is due to the potentiostatic nature that the applied voltage efficiently is transformed into tin dissolution. Galvanostatic processes tend to have lower efficiencies due to oxygen development, hindering the efficiency of the electrolytic process. The 8% losses observed during the two step potentiostatic trails on new scrap are most likely in the form of heat dissipation to the electrolyte caused by its ohmic resistance.

3.3.2. ALLOYED TINPLATE

To determine a rate of tin dissolution from the alloy during the second potential step of -0.2 volt a piece of tinplate that had undergone 24 hours of heat treatment at 250 °C was held at this potential until the current response reached steady state. Figure 3.29 shows the current density response over time of this $FeSn_2$ coated piece of scrap. XRD analysis before the detinning process showed a tin contend of 10.26 and 3.14 gr/m^2, top and bottom respectively. After approximately 45 minutes a steady state seemed to be reached. The tin content afterwards according to the handheld XRF was 0.0 gr/m^2 on both sides. Over three trials the average weight reduction was 0.03155 gram and steady state was reached around 2800 seconds. For $FeSn_2$ with a submerged surface of 28.9 cm^2 held at a potential of -0.2 volt in a 1M NaOH electrolyte at 80 °C the tin stripping rate is 40.5 mg per hour. Figure 3.29 shows the surface of the tin stripped $FeSn_2$ coating. The surface has a brown colour and is porous in nature, as it can be scraped of easily with a sharp edge. The appearance is different compared to the stripped surface of the much thinner layer of $FeSn_2$ on the reflown tinplate, shown in 3.27. As the initial alloy layer was much thicker a more expansive iron atom structure probably forms the porous brown ferric oxide on the surface.

Figure 3.26: Reflown tinplate after the first step

Figure 3.27: Reflown tinplate after the second step

Figure 3.28: Surface of a $FeSn_2$ coating stripped from tin

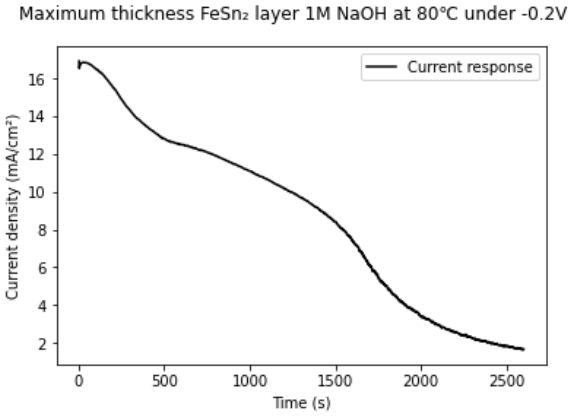

Figure 3.29: $FeSn_2$ coating stripped potentiostatically at -0.2 volt in 1M NaOH at 80°C

3.3.2.1. SEM AND GDOES ANALYSIS

SEM Figure 3.30 shows that visually the process was a success. The top images show the before image, the white color comes from the heavier tin atoms. The white needle like crystalites are not visible after treatment. A porous grey and black surface is visible, indicating that the heavier tin atoms are gone. Some small deposits of white tin is visible in the intermetallic alloy, the treatment did not succeed in a true 100% detinning rate. The bottom image is the after image and shows effective removal of the coating, leaving a tin bearing coating of $0.07\mu m$ thickness. Some porous structure remained on a part of the surface, it is assumed to be very brittle and might have been rinsed off during cleaning. The images speak for the effectiveness of the treatment.

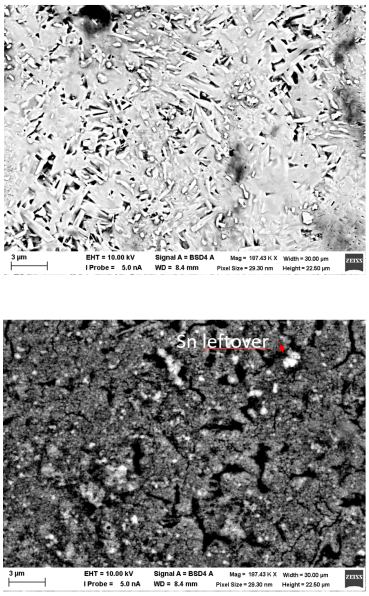

(a) Top profile of the $FeSn_2$ sample

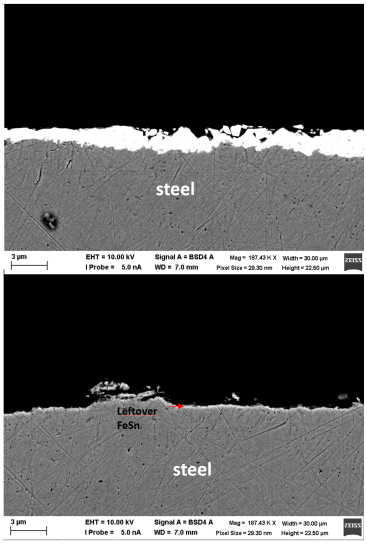

(b) Side profile of the $FeSn_2$ sample

Figure 3.30: SEM images before(top image) and after(bottom image) the detinning process

GDOES "GDOES combines a glow discharge (GD) with an optical emission spectrometer (OES). This is an analytical technique that provides both the surface/depth profile and the bulk elemental composition of solid materials and layers quickly, and with high sensitivity to all elements."[58]. Figure 3.31a shows a weight percentage profile of the untreated $FeSn_2$ sample. the 2:1 ratio is obvious from the depth profile. Figure 3.31b shows the depth profile of the detinned surface of the $FeSn_2$ sample. Note that the depth profile of the oxide on the detinned $FeSn_2$ sample is similar to the tin depth profile. Where tin atoms dissolve, the porous iron structure left behind oxidises. The graphs demonstrate that the tin atom dissolution process is effective, and that porous oxides take the place of these atoms.

Samples were analysed with GDOES, type Horiba Profiler 2. All samples were analysed in duplo. Annex E contains some additional GDOES results comparing $FeSn_2$ and FeSn along with some speculations.

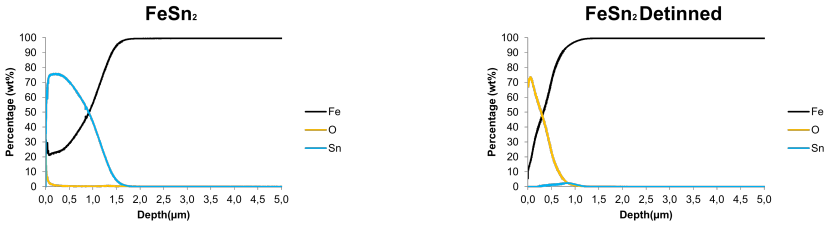

(a) Depth profile $FeSn_2$ coating

(b) Depth profile $FeSn_2$ coating after detinning

Figure 3.31: Weight% depth profile before and after the detinning process

3.3.3. POTENTIOSTATIC RESULTS VS GALVANOSTATIC ELECTROLYSIS

In the industry galvanostatic electrochemical processes are more common than potentiostatic ones. For an galvanostatic electrochemical attack on tin high efficiency is expected, as the current density response is a steady line. As long as there is tin present the response will. Thus if the current density is fixed the potential will change constantly, usually slowly increasing. This makes for a robust process. For $FeSn_2$ and FeSn this is not the case, Figure 3.32 and 3.33 shows schematic with the typical dissolution curve of tin and the alloys as a response to a potential within their respective oxidation window. Both experience a first regime wherein the surface becomes active and remaining oxides are removed. Tin then follows a constant current density value of potential driven dissolution, only limited by tin atom access to the electrolyte. For the tin iron intermetallic alloys the second regime is not limited by the amount of tin surface present, as it does not follow a similar constant current density value but drops gradually. This regime is diffusion limited, and makes up the bulk of the tin dissolution curve of $FeSn_2$ and FeSn during detinning trials. Annex D shows how the duration of the diffusion limited regime is determined.

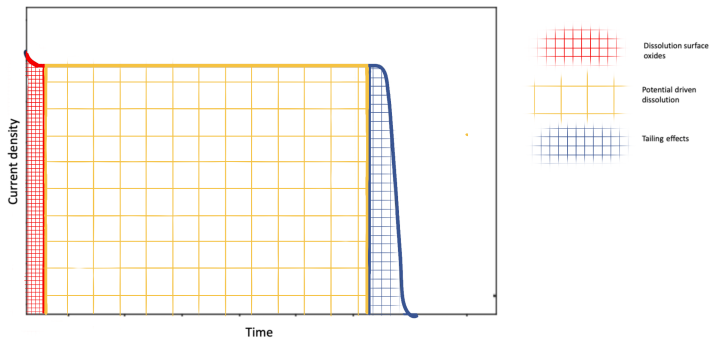

Figure 3.32: Typical shape of the tin dissolution curve at fixed oxidative potential

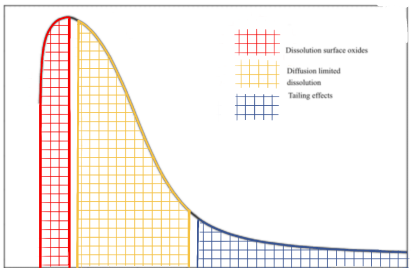

Figure 3.33: Typical shape of the $FeSn_2$ or FeSn dissolution curves at fixed oxidative potential

As some tin is stripped from the alloy the current density response of the system changes, this makes for difficult electrotechnical modeling. So when a fixed current density is applied, and the tin content drops, a lot of energy is wasted on oxygen development instead of tin stripping. Figure 3.34 illustrates these losses if tin-iron alloys would be stripped based on their maximum current density response. As is obvious form the schematic is that a lot of energy would be wasted on oxygen development instead of tin dissolution. If the alloys were to be treated galvanostatically a relatively low current density must be selected for an longer amount of time as seen in Figure 3.35. This would greatly reduce losses to oxygen development, but the duration would increase significantly. Treating the tin-iron alloys on a lower current density would translate in lower energy usage and loss reduction.

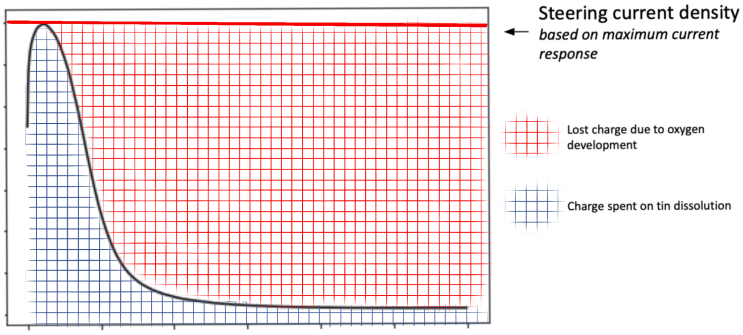

Figure 3.34: Tin-iron alloy galvanostatically treated based on the maximum current density response

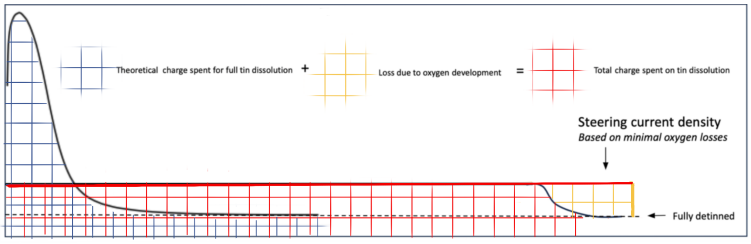

Figure 3.35: Tin-iron alloy galvanostatically treated based on the maximum current density response

3.4. SELECTIVE OXIDATION OF EOL SCRAP

Figure 3.36: Separated steel waste stream form municipal waste

This section of the study will try and apply the previously used two step potentiostatic stripping on EOL scrap to see if similar results will be reached. Figure 3.36 shows a bucket of steel scrap as it would come from a waste separation facility. When observed closely all forms of plastic or paper contamination are present. Almost all scrap seems to have some form of paint or lacquer coating on its surfaces. Matching pieces of scrap have been selected on shape, coating type and tin coating thickness. Of each matching set one piece will be heat treated and the other left as is. By comparing these an assessment can be made of the viability of the potentiostatic process on EOL scrap, and the effect of heat treatment on EOL scrap. Figure 3.37 shows the selected scrap pieces, the right piece of each set has undergone heat treatment of 300 °C for 15 minutes. The selected temperature is based on TJ Crighton his study on alloy formation on tinplate where he concludes: "To ensure maximum recovery of tin from used tinplate, any thermal processing should be limited to temperatures below 350°C and be for as short a time as possible. Processing times will be dependent on the amount of free tin on the surface of the tinplate. All efforts should be made to ensure free tin remains on the surface, otherwise electrolytic recovery of the tin will be jeopardised." The sets of scrap in Figure 3.37 are labeled Set 1, Set 2 and Set 3. Set 1 and Set 2 are made of the same strip, while for Set 3 two matching pieces were selected.

Figure 3.37: Three matching pair of scrap, heat treated pieces on the right side

3.4.1. NON HEAT TREATED PIECES

These trials would represent the treatment of tinplate found in separated municipal steel waste without any prior treatment.

Set 1 The surface of the piece of scrap is different for both sides. The one side has a white coating which already has started to crumble and signs of rust are showing, the tin content on this side is 2.83 gr/m^2. The other side has a 'tin' colored shiny surface without any observable additional coating, its tin contents are 2.62 gr/m^2.

The same two-step electrolytic process used for new scrap has been applied on the end of life scrap. The free tin potential step of -1.0 volt saw a steady current density response, which reached steady state around 80 seconds. The $FeSn_2$ potential step of -0.2 volt saw no current response, which concluded the trial. This piece of scrap was apparently not reflown, as no $FeSn_2$ was present. Afterwards the tin contents were 0.39 gm/m^2 and 0.00 gr/m^2 for the white and uncoated side respectively. The scratched white paint did hinder some of the access of the electrolyte, but still managed to detin the painted surface for 86% and the unpainted surface for 100%.

Set 2 This also has one white side, and one tin coating side. The white coating shows a few scratches where minimal rust is observable. The white side has a tin coating containing 3.5 gr/m^2 of tin, the other side with just tin has a tin content of 2.86 gr/m^2.

During both steps of the process a current density response was observed, which indicates that this piece was reflown. The first step ended after approximately 75 second, while the second took 90 seconds till a steady state was reached. The surface with just a tin coating saw a 100% detin rate as the XRF measured 0.00 gr/m^2. The white paint coating the surface completely hindered the detinning. Measuring the same 3.5 gr/m^2 tin contents as prior to treatment. With some small areas surrounding a scratch measured 3.2 gr/m^2. For non heat treated tinplate this type of painted scrap will not reach any acceptable detin rate.

Set 3 This set has a white coated surface, similar as set 2, with a tin content of 3.81 gr/m^2. The other side has a yellow lacquered surface with a yellowish presumably phenolic based lacquer, with a tin content of 3.15 gr/m^2.

The detin step saw a fluctuating current response quickly reaching a zero steady state, while the $FeSn_2$ step saw no notable current response. After the treatment the white painted side showed a mere 13% detin rate, while the lacquered side 5% to 30% tin reduction depending on the area scanned. No observable scratches were visible in the lacquered side, it is unclear how the electrolyte reached the tin layer.

3.4.2. HEAT TREATED PIECES

During the heat treatment the formation of more $FeSn_2$ is expected, while also causing embrittlement in the paint and lacquer coatings. Hopefully the embrittlement will allow for better access and thus for a better detin rate.

Set 1 After heat treatment the white surface has blackened and has turned very brittle, the tin colored side has become a more dull grey hue. After the short heat treatment tin contents remain at similar values of 2.82 gr/m^2 and 2.59 gr.m^2.

The first potential step showed no current response, indicating that the whole free tin coating has formed $FeSn_2$ with the steel substrate. This was confirmed by the response of the second potential step which lasted for approximately 600 seconds. After treatment the painted side of the tinplate had a tin content of only 0.02 gr/m^2, and the other side was fully detinned at 0.00 gr/m^2. The heat treatment caused the complete free tin layer to alloy into $FeSn_2$, causing a significant increase in duration time. The heat treatment did allow for a better 94% better detinning rate of the painted side for this sample.

It is of note that some folds were observed, which read out higher remaining tin contents than accessible surface. Folds hinder the electrolyte access to fully detin covered areas, a potential solution is further shredding the scrap to liberate the covered surfaces.

Set 2 After the heat treatment the white coated surface has turned a shiny black colour, while the tin coated side has shows minimal change. Tin contents are 3.5 gr/m^2 and 2.85 gr/m^2 respectively.

This sample showed only a very small current density response for the first potential step, reaching steady state in only 15 seconds. Indicating that almost all free tin was alloyed to form $FeSn_2$. After the 0.2 volt potential step the uncoated surface showed a 93% reduction of tin contents. while the painted surface only was a 10 to 18% reduction.

Figure 3.38 showed the pieces of scrap after treatment. Top is the EOL scrap as is, bottom has been heat treated. Both exhibit the yellow ferric oxide color on the detinned surface, which is associated with the detinned $FeSn_2$ alloy.

After the heat treatment this paint still hindered the electrolyte to access the tin. As an experiment the painted surface was scratched to increase the electrolyte access, and was further held at -0.2 volt for 600 seconds. This seemed to have a positive effect, reaching a 45% tin reduction compared to the initial state. But did not fully allow access to the unscratched areas.

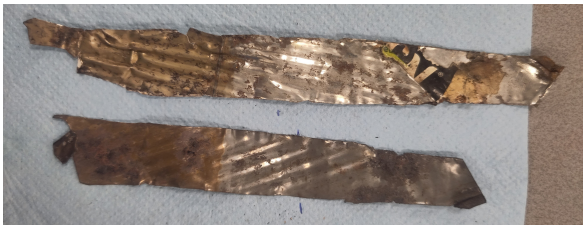

Figure 3.38: Set 2 after detinning. the bottom piece has undergone heat treatment

Set 3 The heat treated piece showed that the white coating turnedFa into the same glossy black shine as Set 2, and has a tin content of 2.84 gr/m^2. The yellow lacquer

turned into a blackish yellow hue, the measured tin content was 2.87 gr/m^2.

During both applied potential steps a fluctuating current density response was observed. As the sample surface is fully coated by paint and lacquer the electrolyte has trouble reaching tin, causing the fluctuating response. Once steady state was reached around 300 seconds the white painted side showed a reduction of 30%, as still tin content of 2,01 gr/m^2 was measured. The lacquered side showed only a 3% decrease of tin contents. The lacquered surface has the worst detin rate observed in the trials. This is problematic as a lot of the tinplate products undergo lacquering.

3.4.3. SUMMARY

Tinplate without a paint or lacquer coating can easily be undone of tin, with detinning rates of 90%+. With the two step potentiostatic method, both heat treated and normal EOL scrap can be fully detinned. The heat treatment applied caused almost all tin present to transform into $FeSn_2$. This is unwanted as tin dissolution from the alloys is significantly slower than from the free tin coating. Future heat treatment experiments should be done for a shorter amount of time. Lowering the temperature would help prevent alloy formation, but also would not succeed to remove most organic burden. Even though the heat treatment already exceeds ideal duration, the treatment is not able to show adequate removal of paints and lacquer coatings. Only for Set 1 an increase was observed, but the paint layer was already damaged and flaky beforehand.

In the trials with EOL scrap the factor that hinders the detinning rate the most is the paint and lacquer coating on the scrap. These coatings hinder the electrolyte to come into contact with the tin coating. Scratching the coatings showed an improvement in tin removal, but still does not allow the electrolyte to fully access the underlying tin bearing coating.

3.5. INDUSTRIAL APPLICATION

The electrochemical behaviour of Tin, blackplate, $FeSn_2$ and FeSn has been studied at lab scale, and on clean and EOL scrap a suitable detinning process has been tested and reviewed. This section discusses some key points that must be considered for the bigger picture of detinning process.

3.5.1. ROLE OF LACQUER

As seen previously the biggest factor hindering the detinning rate of EOL scrap is the presence of lacquer and paint. The temperatures for heat treatment are limited to the $FeSn_2$ formation. At this temperature the lacquers and paint are not weakened or embrittled for sufficient electrolyte access to the tin coating surface.

The standard of lacquer removal at TATA steel described in '00039801-R&D handleiding Lakverijdering van verpakkingstaal'. The most used method to remove lacquer is by immersing the lacquered tinplate in a strong alkaline solution. Similarly a patent from the 1980's claims that the best way to remove paint on tinplate scrap is also to use a strong sodium hydroxide solution[59].

To obtain any significant results for EOL tinplate scrap with coatings such as paint or lacquer a prerequisite 'soaking' bath in NaOH is needed. Both sources call for long periods to fully soften these disruptive coatings. Thus an 8 hour softening batch in heated NaOH must proceed the detinning trials. Such a long soak will also leach remaining free tin of the surface of heat treated tinplate, only calling for an attack on the $FeSn_2$ alloy. This simplifies the process drastically from a electrotechnical point of view.

3.5.2. POSSIBLE ADDITIVES

The performance of the detinning process can be improved by adding additives into the electrolyte in order to favour the tin dissolution and its subsequent deposition on the cathode. Oxidants such as nitrite, persulphate or simple air blowing can aid to the anodic oxidation or tin dissolution [19]. Or additives as $Na_2SnO_3 * H_2O$ limits side reactions and Na_2CO_3 counteracts the initial rapid decrease in NaOH concentration due to the dissolution of tin ions in the solution [60]. To aid the electrochemical alloy attack no additives have been found to increase the tin oxidation out of the alloy[19]. Other additives such as surfectants can influence the deposit structure in a positive manor. If further industrial trials are being done in acidic media, additional tests with iron corrosion inhibitor could prevent steel substrate losses. An example of this is are Organophosphonates, which are stable and efficient [61].

3.5.3. TIN RECOVERY FROM ANODE

Under electrolytic conditions the cathodic reaction of the dissolved tin at the cathode is the following:

$$Sn(OH)_6^{2-} + 4e^- \rightarrow Sn + 6OH^- \tag{3.3}$$

After the tin is dissolved from the anode first it will build up to a certain concentration in the electrolyte, before depositing on the cathode. If the Sn (IV) concentration in the alkaline solution exceeds a certain value (0.5–0.75 g/dm3), tin will be deposited at the cathode in a spongy form[60]. This is desirable because a spongy deposit can be easily scraped of from the cathode plate by scraping. Figure 3.40 on the next page shows the process of cathode scraping at the Nederlandse Onttin Fabriek in Leeuwarden.

After the detinning trials on new and EOL scrap where a stainless steel cathode was used a similar deposit was observed which could easily be scraped off with a sharp edge. This is shown in Figure 3.39a. SEM imaging in Figure 3.39 shows a spongy structure due to the dendritic growth, typical of stannite ions deposition[60].

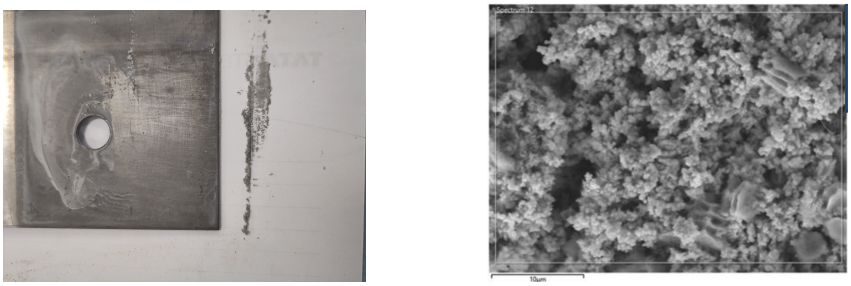

(a) Tin deposition on stainless steel cathode (b) SEM image of tin deposit micro structure

Figure 3.39: Tin deposit after detinning trials [45]

(a) Cathode is charged into machine

(b) Scraper is put into position

(c) Scraping in process

(d) Tin deposit is pressed into cilindrical blocks

Figure 3.40: Cathode scraping and tin block forming process of the NOF

3.5.4. PLANT DESIGN CHOICE

When designing a plant there is a consideration to be made in the plant design to make the process continuous or batch based. While a batch based process is a lot more robust and simple in design, the through put might be less than a continuous operation which also needs less labour. The electrolyte concentration should be very strong. Especially if the same electrolyte is used for the 'soaking' step to soften chemical coatings and leach remaining free tin, literature call for electrolytes with a concentration of 2 to 2.5 molar NaOH[19] [62]. To attack an alloy, a temperature of 75 °C or higher is required. With a small safety margin the operating temperature is chosen at 80 °C. Once heated to that temperature, the operating temperature will remain constant due to the ohmic losses incurred during the detinning [19]. If it for some reason would drop below 80°C, additional heating is required.

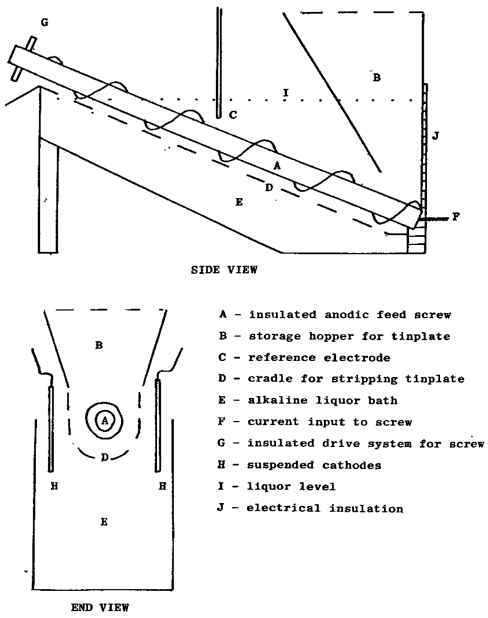

Figure 3.41: Schematic of a concept for a continuous detinning line [19]

Continuous A continuous process has a potential high throughput, yet there are downsides to this process. The system will be a lot more complex, requiring more research and initial investment. More complexity will also lead to an increased chance of process dysfunction as there are more moving parts. One part that has to be removed is the cathode, to recover the deposited tin. This can be disruptive to the process. T.J. Crighton describes it as such[19]: "Removal of the deposited tin requires removal of the cathode altering the charge distribution on a continuous plant, if the current is switched off, rapid dissolution of the reclaimed tin will occur.".

A continuous processing line might reduce the throughput dwell time for clean tinplate by nearly 50%, compared with conventional batch detinning lines, it could also reduce the size of the plant by 50% [19].

A continuous line only makes sense if there is enough available EOL tinplate scrap to sustain a continuous operation. Currently the Dutch municipal solid waste stream for tinplate is not sufficient to supply a large continuous plant.

Batch A batch process is a lot more reliable than a continuous one. The NOF operates a batch process based on multiple smaller cages. During the project we visited the plant and observed the process: The detinning process in which compressed blocks are hung in anode baskets and then placed back into the detinning bath. This setup is part of a cascade configuration, allowing the liquid to flow from high to low through 19 cells connected in series, with a voltage drop across each cell. Each cell contains four baskets, and each basket holds four blocks. A schematic drawing, referred to as Figure 3.42a. After the baskets are positioned, the presence of any short circuit between the anode and cathode is checked by using a crowbar to observe if sparks occur between the anode and cathode. The absence of sparks indicates a short circuit, prompting the repositioning of the basket. During sparking, occasional loud bangs are heard, indicating the production of H2 gas during the detinning process. When inquired about their electrical efficiency, it was reported to be 20%. It was also mentioned that the electric current likely does not reach all areas, implying that detinning occurs in many places through the natural dissolution of tin in NaOH solution, a process significantly slower than electrolytic removal but considered acceptable as the blocks remain in the bath for 21 to 24 hours. The NaOH solution used has a temperature between 70 and 80 degrees Celsius and a molarity of 0.75. because each case has to be filled, lifted out, and emptied separately. This cycle is repeated every 24 hours. This is a very reliable process, but requires around 10 people to operate each cycle change.

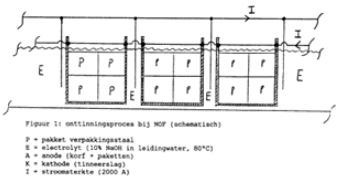

(a) Schematic of a batch detinning line[63]

(b) Batch detinning plant of the NOF

Figure 3.42: Batch electrolysis setup

4

Conclusions and Recommendations

4.1. Conclusions

- The redox behaviour of tin, blackplate, $FeSn_2$ and FeSn has been mapped in cyclic voltagramms for NaOH and MSA electrolyte, as shown in Figures 3.1 and 3.8 respectively. The anodic sweeps in these images determine the active oxidation window.

- The alkaline NaOH electrolyte shows good selectivity. Tin dissolves readily in an alkaline environment. Chrono amperometry shows that a process only dependant on the applied potential which follows a positive relation within the oxidation window. Iron atoms in the blackplate form a passive ferric oxide layer which protects them from dissolution into the electrolyte. The intermetallic alloy $FeSn_2$ is able to be stripped of tin, chrono amperometry shows that this is a process limited by the diffusion layer and electrolyte access to the new surface.

  The acidic electrolyte does not have the desired selectivity for the detinning process. Chrono amperometry shows that the steel substrate dissolve at a faster, and accelerating, rate compared to the tin-iron alloys. Electrolyte will be spent on iron dissolution instead of tin or tin-iron alloys, and the steel product will be lost at a high rate if adequate detinning rate is achieved.

- Cyclic voltametry at elevated temperatures show a significant increase in activity of tin oxidation and reduction at temperatures of 80 °C. It also shows that for an electrolytic attack on the alloys a temperature of 80 °C is required. Chronoamperometry shows that an electrolytic attack on the free tin coating shows steady dissolution until all free tin is depleted. The $FeSn_2$ dissolution does not show a steady dissolution rate and is limited. The tin atoms have to bypass an passive oxide layer. This is limited by the rate of mass transfer. It is also limited by the diffusion boundary layer from tin atoms in the tin-iron alloy surface to the bulk NaOH electrolyte. FeSn is thought to be limited by a

high iron content and thus has a very slow detinning rate, not suitable for a industrial process. Due to the high presence of iron, once the top layer of the alloy coating is stripped of tin, the remaining iron atoms form a passive oxide layer which protect the remainder of the tin atoms remaining in the alloy.

- For the free tin coating a potentiostatic electrolytic attack of applying -1.0 volt would yield high detinning rates. Galvanostatically the current density must be limited 158.7 mA/cm^2 to maximize productivity and economic profit[45]. For $FeSn_2$ a potentiostatic electrolytic attack of -0.2 Volt yields an energy effective detinning rate of 90+%. It is significantly slower than dissolution of a free tin coating but can result in similar detinning rates. A galvanostatic electrolytic attack is possible but with lower efficiency as the dissolution of tin from $FeSn_2$ does not follow a steady dissolution profile but is diffusion limited. A low current density value in the order of 5 mA/cm^2 is advised for an extended amount of time.

- A schematic of a potential detinning line is shown in 4.1. The EOL tinplate will first be heat treated to remove organic burden such as grease, then the heat treated tinplate will first be 'soaked' in NaOH for up to 8 hours to soften lacquer and paint coatings. In the pre-soak bath mechanical agitation will be used to further scratch and remove the chemical coatings. This pre-soak should also be sufficient to leach all the free tin coating that remains after the heat treatment. This allows for a simple one step electrolytic treatment only focusing on the $FeSn_2$ alloy. Potentiostatic treatment would apply a -0.2 volt potential, while the more common galvanostatic approach would apply a low current density of around 3-5 mA/cm^2. If the pre-soak bath and the de-$FeSn_2$ bath are connected and the electrolyte is pumped around, the leached free tin can be recovered at the cathode of the de-$FeSn_2$ step. The electrolytic attack can be done with a continuous or batch plant design, depending on initial investment as well as availability of EOL tinplate scrap. In the current scrap market the tinplate waste stream is not sufficient to warrant the larger upfront investment associated with a continuous process plant.

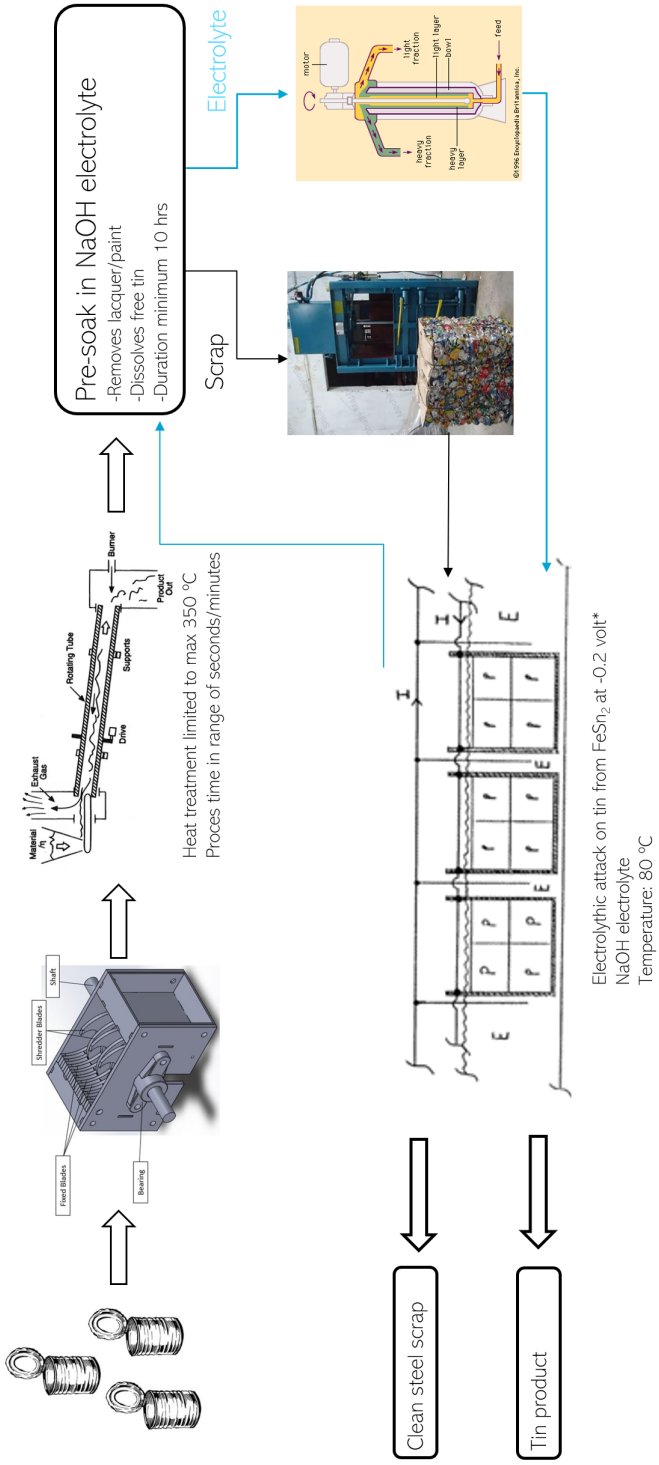

Figure 4.1: Schematic example of a detinning line for EOL tinplate.

4.2. RECOMMENDATIONS

- MSA with additives that prevent iron dissolution should be tested as electrolyte choice. Or other organic acids with a good tin solubility should be tested, eg: Trichloroacetic acid .
- The heat treatment temperature and duration should be studied to found a suitable process to minimise alloy formation while also combating the organic burden.
- One of the big downsides of EOL scrap is that the input is very heterogeneous, and that the composition is unknown. The separated steel solid waste stream should be analysed further to find average values for tin coating thickness, as it influences the optimal heat treatment and electrolytic attack time.
- A deeper look into the to the kinetics and electrochemistry of tin and tin-iron alloy dissolution in alkali electrolyte.
- Advanced sorting/separation techniques at an industrial scale should be researched. Eg; XRF scanning on tin content to devide the steel solid waste stream into tinplate and non tinplate streams.
- Optimal cathode distance should be studied before finalizing the plant design to maximise deposition.
- A range of oxidising agents should be tested to see the effect on tin dissolution from tin-iron alloys.

BIBLIOGRAPHY

[1] Worldsteel. *World Steel in Figures 2022 - worldsteel.org*. Aug. 2022. URL: https://worldsteel.org/steel-topics/statistics/world-steel-in-figures-2022/.

[2] N. Pelletier. "Life Cycle Thinking, Measurement and Management for Food System Sustainability". In: *Environmental Science amp; Technology* 49.13 (June 2015), pp. 7515–7519. DOI: 10.1021/acs.est.5b00441. URL: http://dx.doi.org/10.1021/acs.est.5b00441.

[3] D. Herring. | *Industrial Heating*. Oct. 2014. URL: https://www.industrialheating.com/articles/91892-tramp-elements-and-their-influence-on-steel-and-steel-heat-treatment.

[4] *Tramp Element (Trace) - Engineering Dictionary - EngNet*. URL: https://www.engnetglobal.com/tips/glossary.aspx?word=Tramp+Element+(Trace).

[5] S. Dworak, H. Rechberger, and J. Fellner. "How will tramp elements affect future steel recycling in Europe? – A dynamic material flow model for steel in the EU-28 for the period 1910 to 2050". In: *Resources Conservation and Recycling* 179 (Nov. 2021), p. 106072. DOI: 10.1016/j.resconrec.2021.106072. URL: https://doi.org/10.1016/j.resconrec.2021.106072.

[6] M. C. Friant, W. J. Vermeulen, and R. Salomone. "Analysing European Union circular economy policies: words versus actions". In: *Sustainable Production and Consumption* 27 (July 2021), pp. 337–353. DOI: 10.1016/j.spc.2020.11.001. URL: https://doi.org/10.1016/j.spc.2020.11.001.

[7] | *Industrial Heating*. URL: https://www.industrialheating.com/articles/91892-tramp-elements-and-their-influence-on-steel-and-steel-heat-treatment.

[8] A. Ciocan and F. Potecaşu. "Scrap Quality and Metallurgical Effects Associated with Copper and Tin as Tramp Elements in the Casting Steels". In: *The Annals of "Dunarea de Jos" University of Galati. Fascicle IX, Metallurgy and Materials Science* 33.3 (Sept. 2010), pp. 22–27.

[9] X. Zhang, G. Ma, M. Liu, and Z. Li. "Removal of Residual Element Tin in the Ferrous Metallurgy Process: A Review". In: *Metals* 9.8 (July 2019), p. 834. DOI: 10.3390/met9080834. URL: https://www.mdpi.com/2075-4701/9/8/834/pdf?version=1564999962.

[10] Eurofer. *Steel and the circular economy*. Nov. 2015. URL: https://www.eurofer.eu/assets/Uploads/20151016_CircularEconomyA4.pdf.

[11] E. AISBL. *Metal Recycling Factsheet*. URL: https://euric-aisbl.eu/images/Position-papers/euricmetalrecyclingfactsheet.pdf.

[12] B. of International Recycling. *WORLD STEEL RECYCLING IN FIGURES 2017 – 2021*. 2022. URL: https://www.bir.org/images/BIR-pdf/Ferrous_report_2017-2021_lr.pdf.

[13] *EUR-Lex - 52020DC0098 - EN - EUR-Lex*. URL: https://eur-lex.europa.eu/legal-content/EN/TXT/?qid=1583933814386&uri=COM:2020:98:FIN.

[14] *wetten.nl - Regeling - Besluit beheer verpakkingen 2014 - BWBR0035711*. Apr. 2023. URL: https://wetten.overheid.nl/BWBR0035711/2023-04-19.

[15] T. Crichton and J. Farr. "The Effect of Heat Treatment on the Fe—Sn Alloy System". In: *Transactions of The Institute of Metal Finishing* 82.5-6 (Jan. 2004), pp. 169–173. DOI: 10.1080/00202967.2004.11871585.

[16] C. Dissemination of IT for the Promotion of Materials Science. *Tin can processing*. URL: https://www.doitpoms.ac.uk/tlplib/recycling-metals/tin_cans.php.

[17] J. X. Lu. *Biochemistry, Dissolution and Solubility*. Sept. 2022.

[18] *NEN-EN 10202:2022 en*. URL: https://www.nen.nl/nen-en-10202-2022-en-293459.

[19] T. Crichton. "The Structure and Properties of Tinplate ". In: *University of Birmingham Research Archive e-theses repository* (Nov. 1980).

[20] C. Bertou. *Brit. Pat. 1739, Hydrochloric acid with nitrates, chlorates or other suitable oxidants added is used to attack tinplate*. 1872.

[21] C.B.Schultze. *Fr. Pat. 832 285, HCL iron(iii) dissolution inhibitor*. 1938.

[22] G.Milo. *U.S. Pat. 2 842 435,Add hydrochloric acid to tinplate, and then convert to a galvanic cell by insertion of a zinc rod to act as one electrode and tinplate the other*. 1958.

[23] A. Gutensohn. *Brit. Pat. 1901, Dissolve tin in hydrochloric acid until the liquor is spent, and then add HNO3 or KCIO3 until remainder dissolved*. 1877.

[24] M.Adam. *Brit. Pat. 154 242, Tinplate Is treated in hydrochloric acid and heated In a furnace. Then treated with further hydrochloric acid*$^{t}oremovetinandalloy$. 1919.

[25] E. Edwards. *Brit. Pat. 6803, Tbe use of CU2OCI2 HCI compler copper salt to act as a replenishible oxygen carrier*. 1886.

[26] E. Blundstone. *Brit. Pat. 11 624, Addition of hot solutions of cromium salt to tinplate waste*. 1885.

[27] R. RObinson. *U.S. Pat. 2 208 138, Oxidising effect of persulfate on tinplate in HCL*. 1941.

[28] J. Stevenson. *Can. Pat. 223 600*. 1922.

[29] C. Schultze. *Brit. Pat. 3669*. 1887.

[30] M. Papagianni. *Organic Acids*. Jan. 2011, pp. 109–120. DOI: 10.1016/b978-0-08-088504-9.00011-8. URL: https://doi.org/10.1016/b978-0-08-088504-9.00011-8.

[31] J.W.Hinchley. *Brit, Pat. 346 674, Spongy lead dissolved in excess alkali solution with aid of air or oxygen*. 1930.

[32] A. Gillies. *Australian Pat . 118 756, Tin deposition on stainless steel slabs in alkaline liquor*. 1944.

[33] W. Ballantine. *Brit. Pat. 327 997, Tin recovered by alkaline solution of lead acetate. Alkali added until the white cloud formed Just disappears*. 1929.

[34] C. Zwenger. *Brit. Pat. 3384, Tinned scrap treated with mixture of sodium chloride and sodium hydroxide with some sodium nitrate or manganese dioxide present. The bath is above the melting point of tin*. 1873.

[35] L.Poensgen. *Brit. Pat. 4684, Tin scrap is heated in closed vessel and exposed to action of alkali liquors. The vessel Is rotated, and the resulting ammonia collected*. 1884.

[36] E.Ruf. *U.S. Pat. 1 471 469, Sodium hydroxide liquor with sodium chlorite added, heated to between 50 and 100*^{C}$.Airpassedthroughtheliquor$. 1924.

[37] E.Ruf. *Brit. Pat. 1250 863, An earthenware vessel is filled with tinplate and hydrochloric acid* Once spent, the liquor Is evaporated to yield tin chloride which Is treated with liquid ammonia and copper salts to regenerate the liquor*. 1971.

[38] A. Kissock. *U.S, Pat. 1 501 413, Tin removed by liquor of alkali metal dicbromate in hydrochloric acid at 50-80F*. 1924.

[39] W.C.Gregory. *U.S, Pat.2 229 073, The use of formaldehyde to inhibit acid attack of steel*. 1941.

[40] W. Butterfield. *U.S. Pat. 1 511 967, Tin dissolved In a mixture of B2SO4 , HNO3 and HCl. Stannic oxide washed and reduced to tin*. 1925.

[41] T. Eklund. *Ger. Pat. 512 749, Tin, in the form of sulphide, oxide or chloride, dissolved in hydrochloric acid in presence of oxidising agent*. 1928.

[42] P.Marth. *Fr. Pat, 833 024, Thin costings of caustic alkali applied to, and fused upon, the surface of tin scrap to convert tin to alkali metal stannate*. 1938.

[43] W. S. Jun, P. Yun, and E. Lee. "Leaching behavior of tin from Sn–Fe alloys in sodium hydroxide solutions". In: *Hydrometallurgy* 73.1-2 (Apr. 2004), pp. 71–80. DOI: 10.1016/j.hydromet.2003.08.002. URL: https://doi.org/10.1016/j.hydromet.2003.08.002.

[44] B. Bhattacharyya. *Electrochemical Machining*. Jan. 2015, pp. 25–52. DOI: 10.1016/b978-0-323-32737-4.00002-5. URL: https://doi.org/10.1016/b978-0-323-32737-4.00002-5.

[45] M. Buonincontri. "Electrolytic Removal of Tin from Tinplated Scraps". In: *Politecnico Milano* (2021). URL: https://www.politesi.polimi.it/bitstream/10589/179197/1/2021_10_Buonincontri.pdf.

[46] M.-Y. Li, J. Yang, S. Liang, H. Hou, J. Wang, G. Hu, Z. Li, J. Hu, K. Xiao, and B. Liu. "Ammonia chloride assisted air-chlorination recovery of tin from pyrometallurgical slag of spent lead-acid battery". In: *Resources Conservation and Recycling* 170 (July 2021), p. 105611. DOI: 10.1016/j.resconrec.2021.105611. URL: https://doi.org/10.1016/j.resconrec.2021.105611.

[47] J. Wang, B. Xu, W. Jiang, Y. Li, L. Kong, B. Yang, and H. Xiong. "Development of one-step process method to separate tin from tin-refining sulfur slag via vacuum sulfuration and volatilization". In: *Vacuum* 212 (June 2023), p. 112039. DOI: 10.1016/j.vacuum.2023.112039. URL: https://doi.org/10.1016/j.vacuum.2023.112039.

[48] S. Demcakova, M. Hezelova, and L. Pikna. "SELECTIVE TIN RECOVERY FROM TINNING SLUDGE BY CEMENTATION PROCESS AND CHRONOAMPEROMETRY". In: *Chemical technnology and metalurgy* 56 (Mar. 2021), pp. 603–608.

[49] S. V. Bandekar and P. M. Dhadke. "Solvent extraction separation of tin (IV) with 2-ethylhexyl phosphonic acid mono-2-ethylhexyl ester (PC-88A)". In: *Talanta* (Aug. 1998). DOI: 10.1016/s0039-9140(97)00364-0. URL: https://doi.org/10.1016/s0039-9140(97)00364-0.

[50] J. Qin, S. Ning, J. Xu, F. Guo, Z. Li, Y. Wei, G. Dodbiba, and T. Fujita. "Study on the adsorption behavior of tin from waste liquid crystal display using a novel macroporous silica-based adsorbent in one-step separation". In: *Separation and Purification Technology* 292 (July 2022), p. 121006. DOI: 10.1016/j.seppur.2022.121006. URL: https://doi.org/10.1016/j.seppur.2022.121006.

[51] A. Najjar, M. Orayth, and S. I. Nikitenko. "Separation of tin isotopes using redox ion-exchange chromatography". In: *Polyhedron* 12.7 (Apr. 1993), pp. 791–794. DOI: 10.1016/s0277-5387(00)81760-x. URL: https://doi.org/10.1016/s0277-5387(00)81760-x.

[52] S. T. Amaral and I. Müller. "Electrochemical behaviour of iron in NAOH 0.01 mol/L solutions containing variable amounts of silicate". In: *Journal of the Brazilian Chemical Society* 10.3 (Jan. 1999), pp. 214–221. DOI: 10.1590/s0103-50531999000300010. URL: https://doi.org/10.1590/s0103-50531999000300010.

[53] C. T. J. Low and F. C. Walsh. "Electrodeposition of tin, copper and tin–copper alloys from a methanesulfonic acid electrolyte containing a perfluorinated cationic surfactant". In: *Surface Coatings Technology* 202.8 (Jan. 2008), pp. 1339–1349. DOI: 10.1016/j.surfcoat.2007.06.032. URL: https://doi.org/10.1016/j.surfcoat.2007.06.032.

[54] M. Gernon, M. Wu, B. T. S, and P. K. Janney. "Environmental benefits of methanesulfonic acid". In: *Green Chemistry* 1.3 (Jan. 1999), pp. 127–140. DOI: 10.1039/a900157c. URL: https://doi.org/10.1039/a900157c.

[55] M. Armbrüster, M. Schmidt, R. Cardoso-Gil, H. Borrmann, and Y. Grin. "Crystal structures of iron distannide, FeSn2, and cobalt distannide, CoSn2". In: *Zeitschrift Fur Kristallographie-new Crystal Structures* 222.2 (June 2007), pp. 83–84. DOI: 10.1524/ncrs.2007.0033. URL: https://doi.org/10.1524/ncrs.2007.0033.

[56] T. Xometry. "Alloys: Definition, composition, types, properties, and applications". In: (Apr. 2023). URL: https://www.xometry.com/resources/materials/what-is-an-alloy/#:~:text=Improved%20Properties%3A%20Alloys%20are%20created,corrosion%2Dresistant%20than%20pure%20copper..

[57] *COMPOUND SUMMARY methanesulfonic acid, iron(2+) salt.* URL: https://pubchem.ncbi.nlm.nih.gov/compound/Iron-methanesulfonate.

[58] *What is Glow Discharge Optical Emission Spectroscopy GDOES? - HORIBA.* URL: https://www.horiba.com/int/scientific/technologies/glow-discharge-optical-emission-spectroscopy/glow-discharge-optical-emission-spectroscopy/.

[59] H. Giezen. *EP0105551A1 - Method for the detinning of painted tinplate waste - Google Patents*. Sept. 1982. URL: https://patents.google.com/patent/EP0105551A1/da.

[60] M. Šeruga, M. Metikoš-Huković, T. Valla, M. Milun, H. Hoffschultz, and K. Wandelt. "Electrochemical and X-ray photoelectron spectroscopy studies of passive film on tin in citrate buffer solution". In: *Journal of Electroanalytical Chemistry* 407.1-2 (May 1996), pp. 83–89. DOI: 10.1016/0022-0728(95)04502-3. URL: https://doi.org/10.1016/0022-0728(95)04502-3.

[61] *Scale Control by Acid Addition and Scale Inhibitor Addition.* Mar. 2022. URL: https://www.dupont.com/content/dam/dupont/amer/us/en/water-solutions/public/documents/en/RO-NF-FilmTec-Scale-Control-Acid-Addition-Manual-Exc-45-D01547-en.pdf.

[62] Q. Chen, Z. Ma, R. Ni, and W.-R. Sun. "Removal and retrieval of tin from tinned steel sheet by electrolyzing with caustic solution". In: *Steel research* 69.6 (June 1998), pp. 224–227. DOI: 10.1002/srin.199805540. URL: https://doi.org/10.1002/srin.199805540.

[63] T. Steel. "Electric detinning cell of the NOF". In: *internal document* ().

5

ANNEX

5.1. A: FESN AND $FeSn_2$ SAMPLE TRIALS

Various alloying trials were attempted. Trials using: iron powder and tin pellets, various ratios of tin coating to substrate and additional tin pellets added to tinplate. Argon/hydrogen, nitrogen and airated atmospheres have been tested, resulting in a varuous range of oxides as shown in Figure 5.1. Tin that oxidises wont diffuse to form alloy, thus oxidation must be minimised [15].

Figure 5.1: Various trial attempts to create tin iron alloys

5.2. B: INFLUENCE OF REFERENCE ELECTRODE DISTANCE

Figure 5.2 Shows the importance of the reference electrode distance to the work surface. For an image the least distorted by ohmic drop, the reference electrode must be as close as possible. This shortens the distance ions have to travel through the electrolyte, thus minimising the ohmic resistance of the electrolyte.

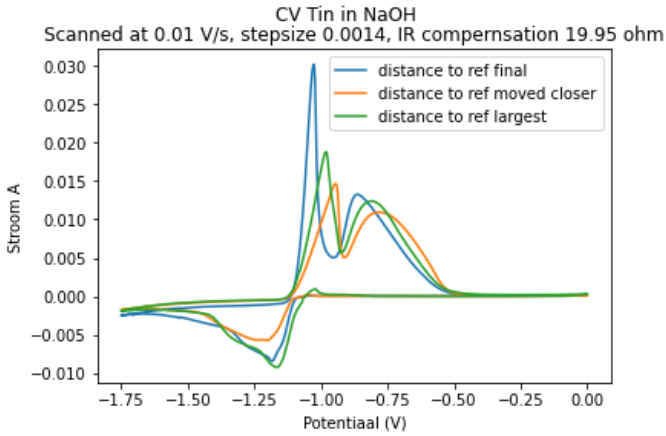

Figure 5.2: Three Cyclic Voltagramms with differnt reference electrode distance

5.3. C: OSCILATION TIN IN NAOH AT ROOM TEMP

Early Cyclic Voltammetry trials showed that in the pure tin in NaOH system there is a difference in the first and second anodic peak. The onset of the first peak never showed oscillation, while the second peak often started oscillating as seen in Figure 5.3. The potential range in the valley of both peaks from -0.98 to -0.78 volt is a considered less stable, the oscillating as result. In this range and under room temperature, dissolved tin want to reduce back onto the surface as tin oxides(Equation 2.2), while tin dissolution from the surface happens at the same time(Equation 2.1). This causes two oscillating reactions seen in Figure 5.3. The oscillating could be combated by setting appropriate scan rate and step size.

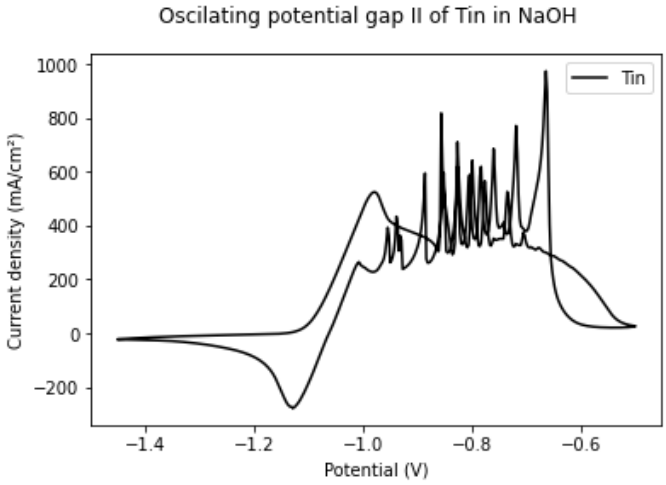

Figure 5.3: Oscillating behavior of peak II of tin at room temperature

5.4. D: DIFFUSION LIMITED REGIME OF TIN-IRON ALLOYS

By comparing a Chronoamperometry measurement vs the same measurement but with the square root time axes, the diffusion limited area becomes clear. Diffusion is a time dependant process, that if the time axes gets rooted, will become linear. Figure 5.4 demonstrates this comparison, highlighting the diffusion limited regime.

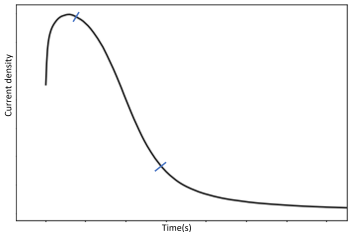

(a) Schematic of a typical tin-iron alloy dissolution curve

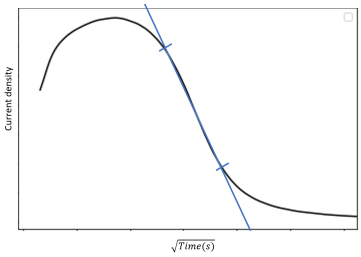

(b) Schematic of a tin-iron alloy dissolution curve against the square root of time

Figure 5.4: W

5.5. E: ADDITIONAL GDOES ANALYSIS

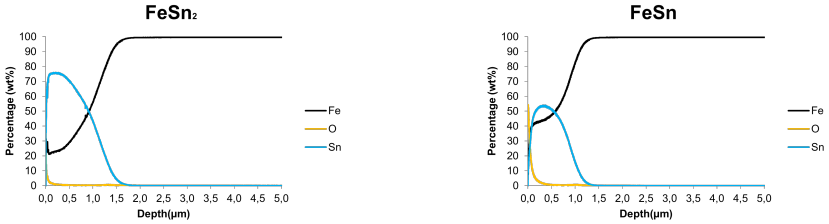

(a) Depth profile of $FeSn_2$

(b) Depth profile of FeSn

Figure 5.5: Weight% depth profile of tin-iron intermetallic alloys

5

Figure 5.5 Shows the weight% depth profiles of both intermetallic alloys. As expected $FeSn_2$ has a higher tin ratio along the depth profile until the $1.0\mu m$ depth. FeSn is only sees a slightly higher tin content until $0.65\mu m$, until this point the tin iron ration is close to 50%. From here iron is more prevalent, and the tin atoms will have to surpass more iron oxide barriers. Figure 5.6 shows the same graphs but have a red highlighted area of the depth profile where tin is more prevalent than iron. For $FeSn_2$ a substantial part of the depth profile the tin content, this area represents tin atoms are not/less hindered by iron oxide barriers. For FeSn this is a small area, from an early depth the tin atoms must overcome these barriers.

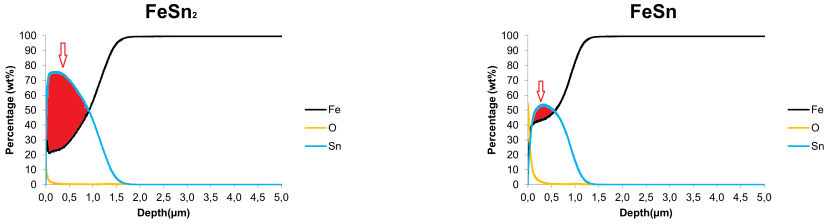

(a) Marked in red the depth where tin exceeds iron content

(b) Marked in red the depth where tin exceeds iron content

Figure 5.6: Highlighted weight% depth profile of tin-iron intermetallic alloys